GPO PRICE $ _____

CFSTI PRICE(S) $ _____

Hard copy (HC) $3.00

Microfiche (MF) .50

ff 653 July 65

NASA CR-54918

MEASUREMENT OF THE PERMEABILITY OF TUNGSTEN TO HYDROGEN AND TO OXYGEN

Final Report

by

E. A. Aitken, P. K. Conn, E. C. Duderstadt, and R. E. Fryxell

prepared for

NATIONAL AERONAUTICS and SPACE ADMINISTRATION

Contract No. NAS 3-6216

NUCLEAR MATERIALS and PROPULSION OPERATION

ATOMIC PRODUCTS DIVISION

GENERAL ELECTRIC

Cincinnati, Ohio 45215

NOTICE

This report was prepared as an account of Government sponsored work. Neither the United States, nor the National Aeronautics and Space Administration (NASA), nor any person acting on behalf of NASA:

A.) Makes any warranty or representation, expressed or implied, with respect to the accuracy, completeness, or usefulness of the information contained in this report, or that the use of any information, apparatus, method, or process disclosed in this report may not infringe privately owned rights; or

B.) Assumes any liabilities with respect to the use of, or for damages resulting from the use of any information, apparatus, method or process disclosed in this report.

As used above, "person acting on behalf of NASA" includes any employee or contractor of NASA, or employee of such contractor, to the extent that such employee or contractor of NASA, or employee of such contractor prepares, disseminates, or provides access to, any information pursuant to his employment or contract with NASA, or his employment with such contractor.

NASA CR-54918

Final Report

MEASUREMENT OF THE PERMEABILITY OF TUNGSTEN TO HYDROGEN AND TO OXYGEN

by

E.A. Aitken, P.K. Conn, E.C. Duderstadt, and R.E. Fryxell

prepared for

NATIONAL AERONAUTICS and SPACE ADMINISTRATION

May, 1966

Contract No. NAS3-6216

Technical Management
NASA Lewis Research Center
Cleveland, Ohio
Materials and Structures Division
Richard E. Gluyas

NUCLEAR MATERIALS and PROPULSION OPERATION
ATOMIC PRODUCTS DIVISION
GENERAL ELECTRIC
Cincinnati, Ohio 45215

MEASUREMENT OF THE PERMEABILITY OF TUNGSTEN TO HYDROGEN AND TO OXYGEN

by

E.A. Aitken, P.K. Conn, E.C. Duderstadt, and R.E. Fryxell

ABSTRACT

Permeation rates of hydrogen through arc-cast tungsten were measured at temperatures from 1300° to 2600°C with hydrogen pressure differentials of 1 and 0.1 atmospheres across isothermal membranes. Rates were nearly proportional to square root of pressure, were inversely proportional to membrane thickness, and had an activation energy of 33 kcal/mole.

Permeation rates of oxygen through tungsten were studied in the temperature range 2000° to 2600°C. Sealed tungsten capsules containing known quantities of tungsten oxide were tested in helium and hydrogen, then broken open and the remaining oxygen assayed. Permeation coefficients obtained in this manner had a temperature dependency in the range of 40 to 45 kcal/mole.

CONTENTS

FIGURES

TABLES

SUMMARY

Permeation rates of hydrogen through arc-cast tungsten were measured at temperatures from 1300° to 2600°C with hydrogen pressure differentials of 1 and 0.1 atmospheres across isothermal membranes. Rates were nearly proportional to square root of pressure, were inversely proportional to membrane thickness, and were temperature dependent according to the equation:

$$P = 33.2 \exp(-33,000 \pm 1000/RT)$$

where:

P = permeation coefficient in cc (STP)-mm/cm^2-min-atm$^{1/2}$
R = gas constant in calorie/mole-°K
T = absolute temperature in °K

Permeation rates of oxygen through tungsten were studied in the temperature range 2000° to 2600°C. Sealed tungsten capsules containing known quantities of tungsten oxide were tested in helium and hydrogen, then broken open and the remaining oxygen assayed. A permeation coefficient was calculated for each capsule based on test conditions, initial and final oxygen contents, and oxygen pressures calculated from equilibrium constants for dissociation of tungsten oxides. Permeation coefficients obtained in this manner had a temperature dependency in the range of 40 to 45 kcal/mole.

MEASUREMENT OF THE PERMEABILITY OF TUNGSTEN TO HYDROGEN AND TO OXYGEN

INTRODUCTION

The purpose of this investigation was to determine experimentally the permeabilities of hydrogen and oxygen through polycrystalline tungsten at temperatures ranging from 1500° to 2600°C. Permeation rates of hydrogen through tungsten have been measured at temperatures up to 925°C,[1,2] but no previous measurements have been reported for the temperature range covered in this investigation. Some diffusion measurements[3,4] and solubility measurements[3] have been made at temperatures below 2200°C. No previous permeability studies of oxygen through tungsten are known to the authors; however, efforts have been made to determine diffusion rates[5-7] and solubilities.[8,9]

Permeation has been defined by Norton[10] as the over-all steady state flow process from the gas phase on one side of a membrane or wall to the gas phase on the other side. Several steps are involved in the process:

1. Impact of the gas atoms or molecules on the surface.
2. Adsorption.
3. Possible dissociation upon adsorption.
4. Solution of the gas in the wall material at the incoming surface.
5. Movement of the gas atoms from this saturated surface layer through the interior as atoms or ions, under a concentration gradient, to the outgoing surface (diffusion).
6. Exsolution of the dissolved gas to the outgoing surface layer with possible recombination.
7. Desorption.

For diatomic gases, which dissociate prior to diffusion, the quantity of gas which permeates through a membrane or wall at a given temperature is directly proportional to the surface area of the membrane, the length of time of permeation, and the difference between the square roots of the pressures on each side of the membrane, and it is inversely proportional to the thickness of the membrane, thus:

$$q = P A t (p_1^{1/2} - p_2^{1/2})/d \qquad (1)$$

where:

q = total amount of gas permeating a membrane
P = temperature dependent permeation coefficient
A = area of membrane exposed
t = time
p_1 = gas pressure of high pressure side
p_2 = gas pressure of low pressure side
d = thickness of membrane

When the surface reactions are not rate controlling steps, the permeation coefficient, P, is equal to the product of diffusivity and solubility. The permeation coefficient is also temperature dependent according to the equation:

$$P = P_0 \exp(-Q/RT) \quad (2)$$

where:

P_0 = permeation constant
Q = activation energy
R = gas constant
T = absolute temperature

Materials and experimental procedures used in this investigation and the results obtained are included in this report. The various types of tungsten and the gases used in this work are described in Appendix A.

EXPERIMENTAL PROCEDURES

Hydrogen Permeation

Permeation rates of hydrogen through arc-cast tungsten were measured at temperatures from 1300° to 2600°C using the permeation cells shown in Figures 1 and 2. Each cell consisted of two cylindrical chambers separated by a 0.26- or a 0.53-mm-thick membrane fabricated from wrought tungsten sheet made from vacuum arc-cast tungsten. Membranes were electron beam welded to the two arc-cast tungsten tubing segments simultaneously. The tungsten-molybdenum-rhenium alloy envelopes of cell 2 had previously been electron beam welded to the tungsten tubing segments, and the molybdenum end caps with Mo tubes (and small W-Re inner extension tubes) were TIG welded to the W-Mo-Re envelopes last. Tungsten-molybdenum-rhenium end caps with short lengths of W-Mo-Re tubes and W-Re inner extension tubes had previously been electron beam welded to the ends of the heavy walled tungsten segments of cells 3 and 4. Small Mo tubes were TIG welded to the W-Mo-Re tubes last. Cell 1 (not shown) was similar to cell 2 except that it did not contain the small W-Re inner extension tubes. Cell 1 developed leaks during testing, and although reliable permeation coefficients were not obtained, it was very useful in the selection of test conditions for the other cells.

Particular attention to weld joint design and material selection was necessary to obtain leak-free welds. All cells were leak-free as determined with a helium mass spectrometer leak detector before they were used for permeation measurements; cells 2, 3, and 4 were leak-free after test as determined in the same manner.

The permeation cells were mounted vertically in a high temperature tungsten resistance furnace and the membranes and center portions heated to test temperatures. Temperatures were measured using an optical pyrometer sighting on the edge of the membrane through a small hole in a tungsten plate which was fastened to the side of the cell. This arrangement provided an approximate black body condition and eliminated the need for emissivity corrections. Appropriate corrections were made for the quartz window through which the temperatures were measured. Argon gas flowed through the 10 liter volume of the furnace at the rate of 4.7 liters/min. For hydrogen pressure differentials of one atmosphere, hydrogen flowed through one end of the cell at the rate of 250 cc/min (minimum of 10 volume changes per minute), entering through the small W-Re inner extension tube and exhausting to the atmosphere through the other tube. Permeation rate measurements at hydrogen pressure differentials less than one atmosphere were made by diluting the hydrogen with argon to obtain the desired partial pressure. A negligible hydrogen pressure was maintained on the opposite side of the membrane by sweeping argon through that end of the cell at 500 cc/min (minimum of 20 volume changes per minute).

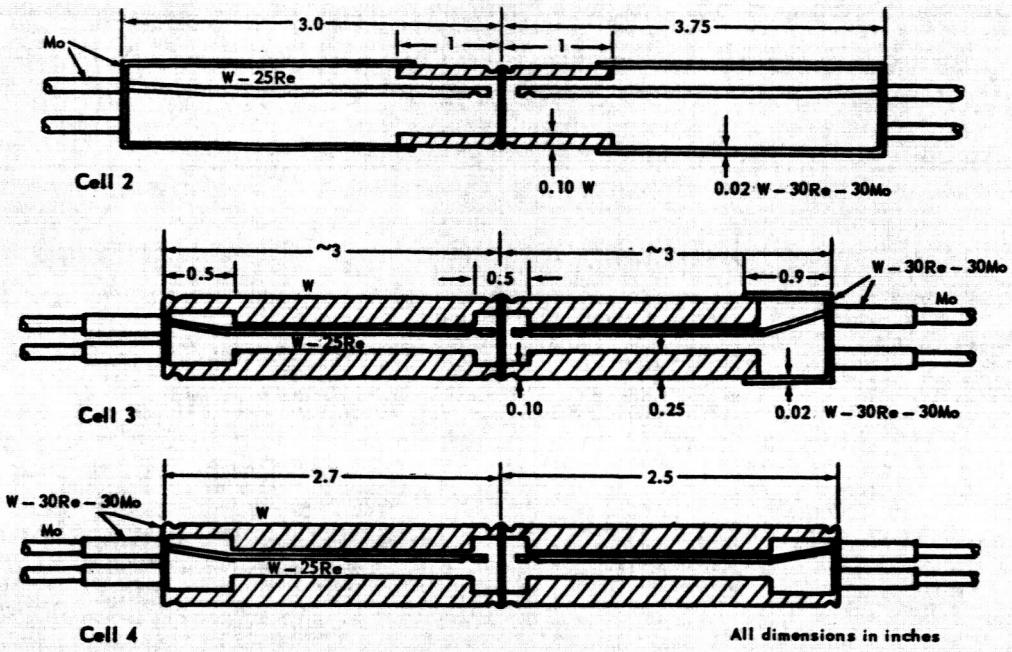

Fig. 1 – Schematic drawing of hydrogen permeation cells

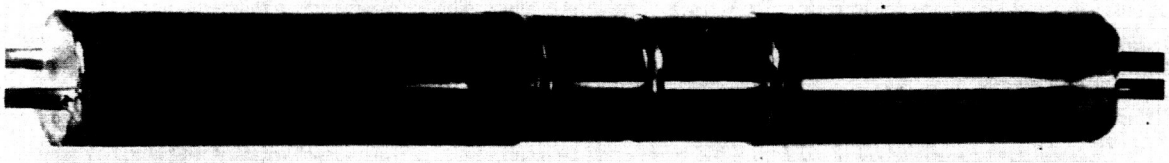

Cell 2 (Neg. P65-12-11A)

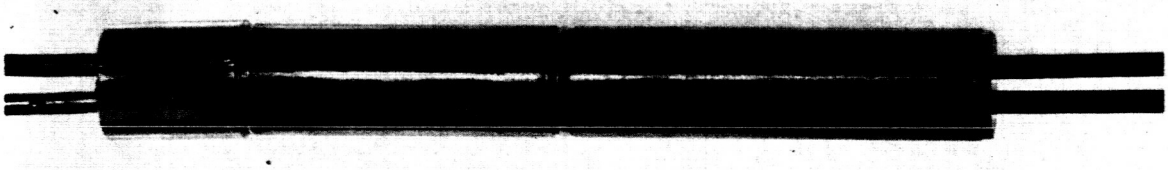

Cell 3 (Neg. P66-1-12)

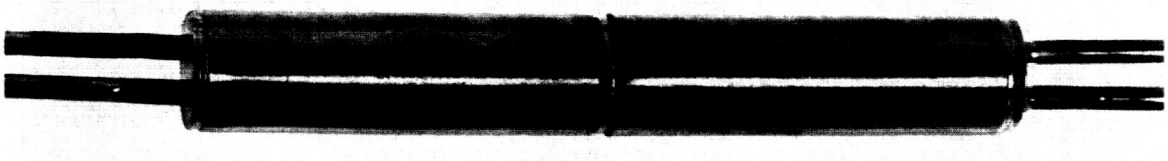

Cell 4 (Neg. P66-2-3)

Fig. 2 – Photographs of hydrogen permeation cells

Hydrogen which permeated through the membrane was carried from the cell via the argon sweep gas and was converted to H_2O by reaction with CuO at 600°C. The H_2O was collected on $Mg(ClO_4)_2$ in bottles which were weighed periodically. The conversion and collection apparatus was calibrated using pure hydrogen at known volume, pressure, and temperature. Four calibration runs were conducted with 100.0 ± 0.7 percent recovery of the H_2O.

Small amounts of hydrogen permeated out through the walls of the hydrogen end of the cell into the furnace argon. This hydrogen was prevented from entering the argon-end of the cell through the walls and affecting the permeation measurements, by positioning the cell in the furnace with the hydrogen end upward and sweeping the furnace-argon upward past the cell. The results of periodic analyses of the furnace-argon (samples taken from the top exhaust line) are given in Table 1 and show that hydrogen partial pressure differentials across the wall of the argon-ends of the permeation cells were sufficiently small that negligible permeation of hydrogen into or out of the exit end of the cell would occur. Cells 3 and 4 were designed with very thick walls to minimize the amount of hydrogen permeating through them.

TABLE 1

COMPARISON OF HYDROGEN CONTENTS OF ARGON SWEEP GAS AND FURNACE ARGON[a]

Temperature, °C	Cell 2 ppm H_2 in[b]		Cell 3 ppm H_2 in[b]		Cell 4 ppm H_2 in[b]	
	Ar Sweep	Furnace	Ar Sweep	Furnace	Ar Sweep	Furnace
1500	30	<50	–	–	–	–
1800	–	–	70	<25	–	–
2000	250	206	100	34	–	–
2400	800	500	400	87	600	55
2500	1000	741	–	–	–	–
2600	1300	788	200[c]	34[c]	1000	99

[a]A difference of 100 ppm H_2 between the sweep gas and the furnace gas corresponds to a pressure differential of 10^{-4} atmospheres.
[b]For 1 atm H_2 pressure differential across the membrane.
[c]For 0.1 atm H_2 pressure differential across the membrane.

Oxygen Permeation

The high volatility of the tungsten oxides at elevated temperatures prohibited the use of permeation cells of the usual design for measurement of oxygen permeation rates since all tungsten parts would quickly be eroded away in a dynamic atmosphere containing oxygen. Therefore, oxygen permeation rates through tungsten were measured using sealed tungsten capsules containing static oxygen bearing atmospheres. These capsules, which contained known quantities of WO_3, were fabricated by electron beam welding tungsten sheet ends to short lengths of tungsten tubing. Partial pressures of O, O_2, and the various tungsten oxides at test conditions were calculated using appropriate thermodynamic data from the literature (see Appendix B). Optimum test temperatures for this technique are 2000° to 2300°C; at temperatures below 1900°C, condensed oxide phases exist under the specific loading conditions used, complicating the problem of defining the oxygen partial pressure in the capsule; at temperatures above 2300°C, test times are too short to be measured accurately unless extremely thick-walled capsules are used.

Specimens were heated in high temperature tungsten resistance furnaces in flowing helium atmospheres. A few tests were conducted in hydrogen. Temperatures were measured optically, sighting on the top surface of the specimen through a small hole in a tungsten plate lying on top of the test specimens. Specimens were leak tested both before and after testing. After testing, specimens were broken open in a device capable of collecting any gases the capsule might contain. The quantity of remaining condensed tungsten oxides

was determined by reheating the specimen fragments ($W + W_xO_y$) in flowing hydrogen to 800° – 1000°C to reduce the W_xO_y to W. The quantity of H_2O obtained from the reaction $W_xO_y + yH_2 \rightarrow xW + yH_2O$ was measured by passing the hydrogen containing this H_2O through an electrolytic hygrometer and integrating its output to obtain total H_2O passing through the hygrometer during the time the reduction reaction occurred. This apparatus was calibrated using known quantities of WO_3 and one untested permeation specimen. Results of calibration runs averaged 97 percent ± 2 percent of that expected. This method of analysis was selected after preliminary experiments showed that the quantity of oxygen lost was sufficiently high to be measured by this technique. In several instances, the amount of oxygen remaining after testing was determined directly from weight loss which occurred during the reduction process. The quantities of oxygen which permeated through the tungsten walls of the specimens were calculated, as shown in Appendix C, from the difference between initial and final oxygen contents. Initial and final O and O_2 pressures from which average pressures were calculated, were obtainable from Figures B1 to B5 in Appendix B.

Adequate quantities of usable 11.7 mm O. D. x 0.5 mm wall tungsten tubing fabricated from arc-cast tungsten could not be procured. That which was obtained was extremely fragile; a large portion of it cracked before and while being cut to length, and many segments which were successfully cut to length cracked while end caps were being welded in place. Because of the paucity of arc-cast tungsten tubing, specimens were also fabricated from electro-deposited tungsten tubing, vapor-deposited tungsten tubing, and crucibles made by powder metallurgy techniques.

RESULTS AND DISCUSSION

Hydrogen Permeation

Steady-state hydrogen permeation rates through the 0.26-mm-thick arc-cast tungsten membranes are shown in Figures 3 and 4, where quantity of hydrogen permeated is plotted versus time for one atmosphere hydrogen pressure differential. Similar data for a 0.53-mm-thick membrane are shown in Figure 5. Permeation rates for 0.1 atmosphere hydrogen pressure gradient across 0.26 mm membranes are shown in Figures 6 and 7. Permeation coefficients calculated from these rates, membrane surface areas and thicknesses, and hydrogen pressures (using equation 1) are summarized in Table 2. Permeation coefficients for a given temperature and cell are listed chronologically in Table 2 and may be related to prior thermal history of the cell by use of Figure 8 which contains a graphical presentation of the thermal histories of the permeation cells.

Coefficients obtained from the three cells are generally in good agreement, with the exception that coefficients obtained from cell 4 at temperatures above 2200°C were somewhat lower than those obtained from cells 2 and 3. In most instances, the agreement between coefficients calculated from 0.1 atmosphere pressure differential data and those from 1 atmosphere pressure differential data is good, demonstrating that the diffusing species is atomic hydrogen. One exception was the 2600°C data from cell 4; in this instance, the lack of agreement between 0.1 and 1 atmosphere data can be resolved using the dissociation data given by Stull and Sinke[11] and assuming equilibrium dissociation of the hydrogen in the cell. However, inasmuch as cells 2 and 3 did not show similar behavior, this difference may not be significant and may be assignable to experimental error.

At 1500°C, the absolute permeation rate at 0.1 atmosphere is so low that the actual moisture content in the argon sweep gas is near the equilibrium vapor pressure of the $Mg(ClO_4)_2$. Thus, the data for cell 2 failed to show the expected square-root-of-pressure dependency; however, this dependency was obtained from the data at 1500°C for cell 4, and a reasonable value of the permeation coefficient was obtained at 1 atmosphere pressure differential at 1300°C.

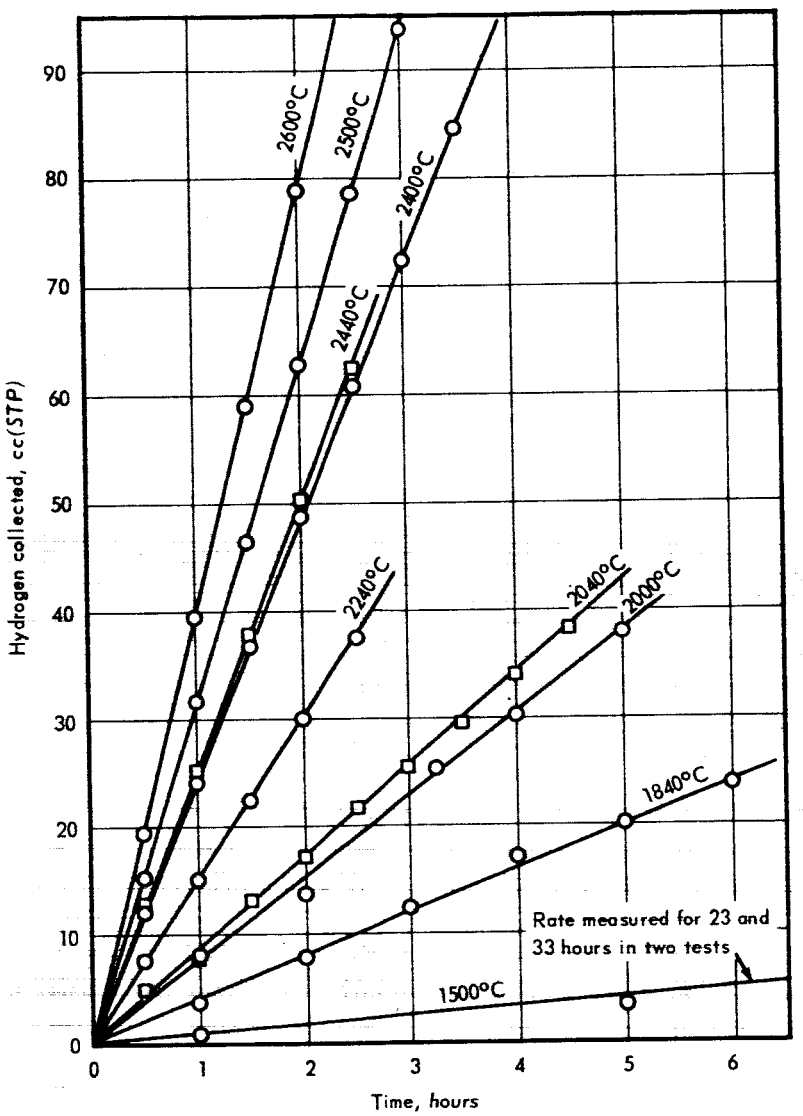

Fig. 3 – Permeation rates of hydrogen through 0.26 mm arc-cast tungsten membrane of Cell 2 with 1 atmosphere hydrogen pressure differential (membrane area = 1.54 cm^2)

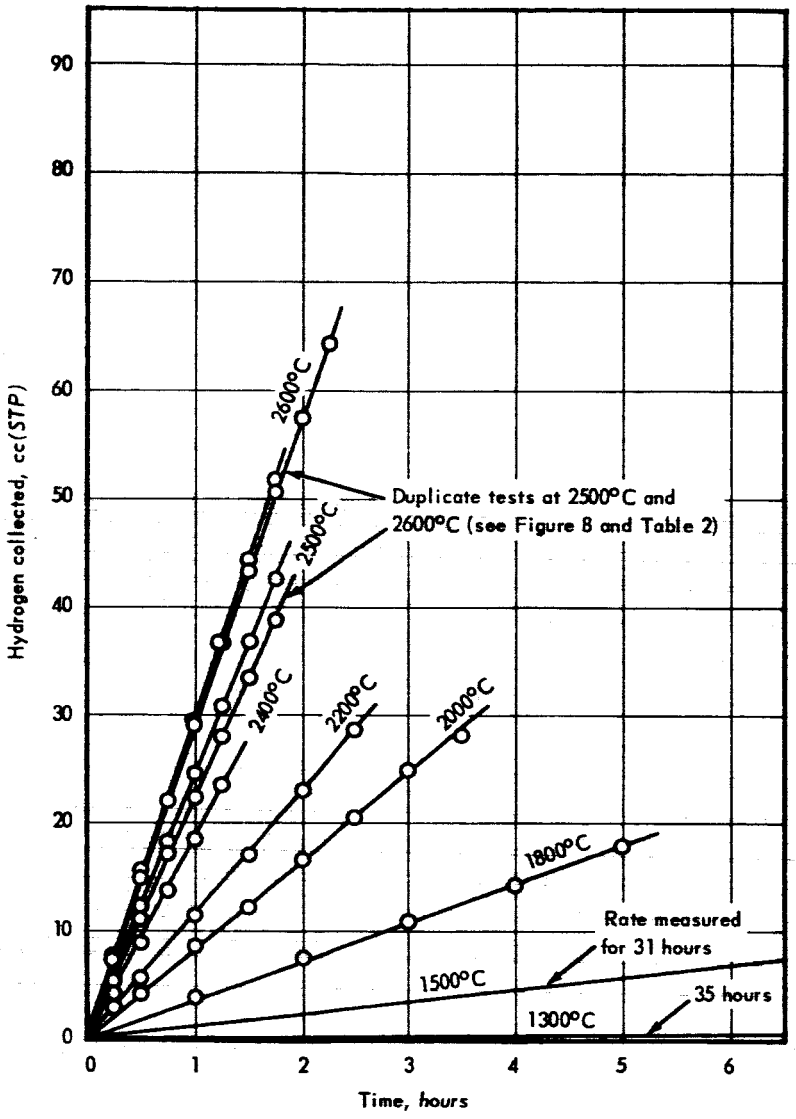

Fig. 4 – Permeation rates of hydrogen through 0.26 mm arc-cast tungsten membrane of Cell 4 with 1 atmosphere hydrogen pressure differential (membrane area = 1.49 cm^2)

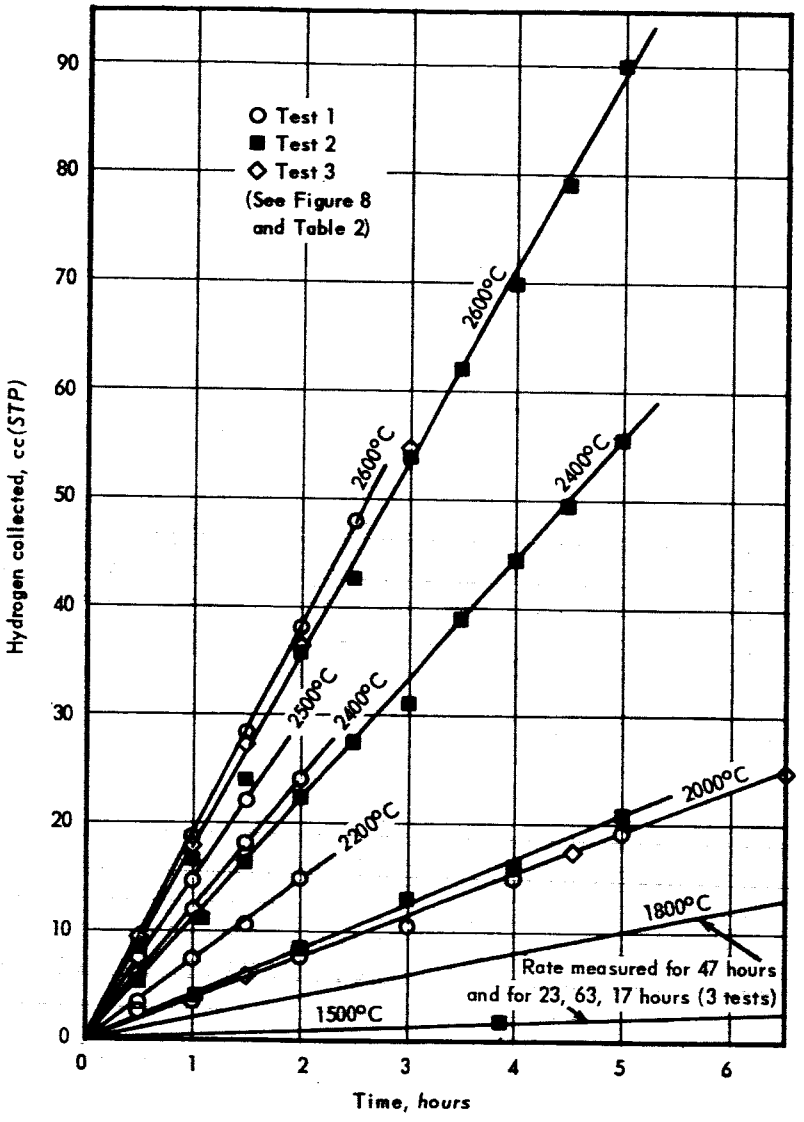

Fig. 5 – Permeation rates of hydrogen through 0.53 mm arc-cast tungsten membrane of Cell 3 with 1 atmosphere hydrogen pressure differential (membrane area = 1.49 cm^2)

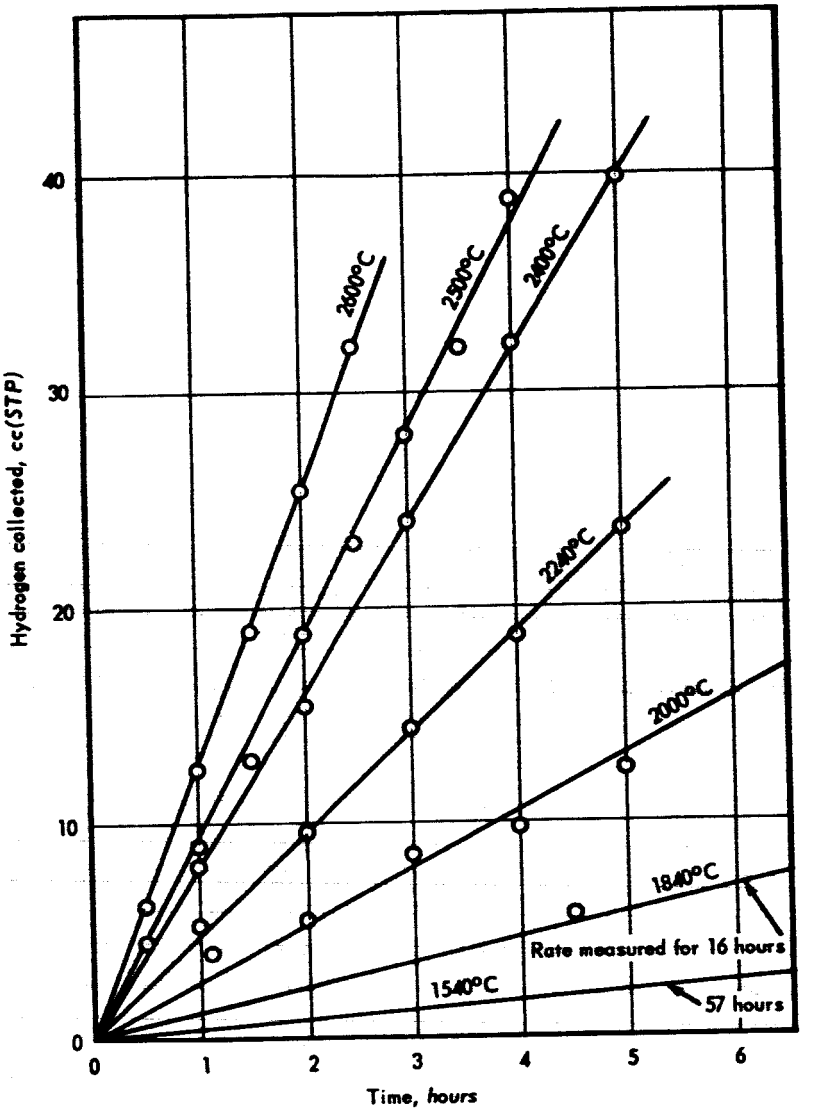

Fig. 6 – Permeation rates of hydrogen through 0.26 mm arc-cast tungsten membrane of Cell 2 with 0.1 atmosphere hydrogen pressure differential (membrane area = 1.54 cm^2)

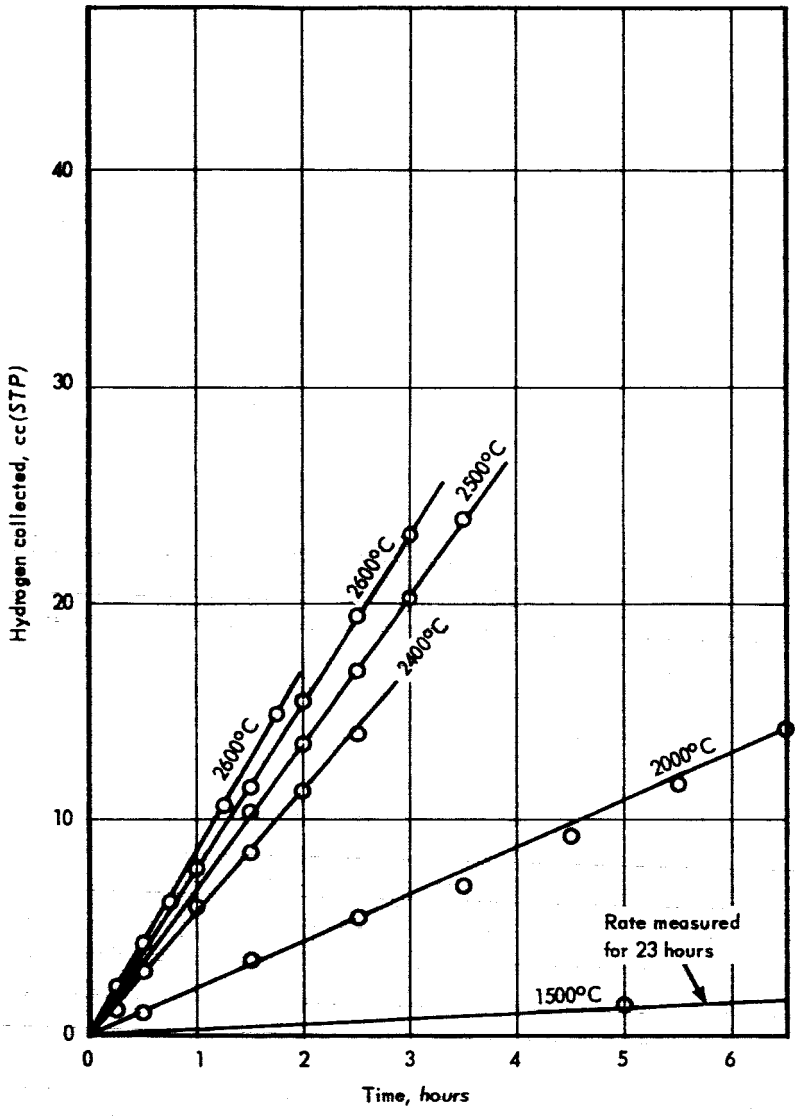

Fig. 7 – Permeation rates of hydrogen through 0.26 mm arc-cast tungsten membrane of Cell 4 with 0.1 atmosphere hydrogen pressure differential (membrane area = 1.49 cm^2)

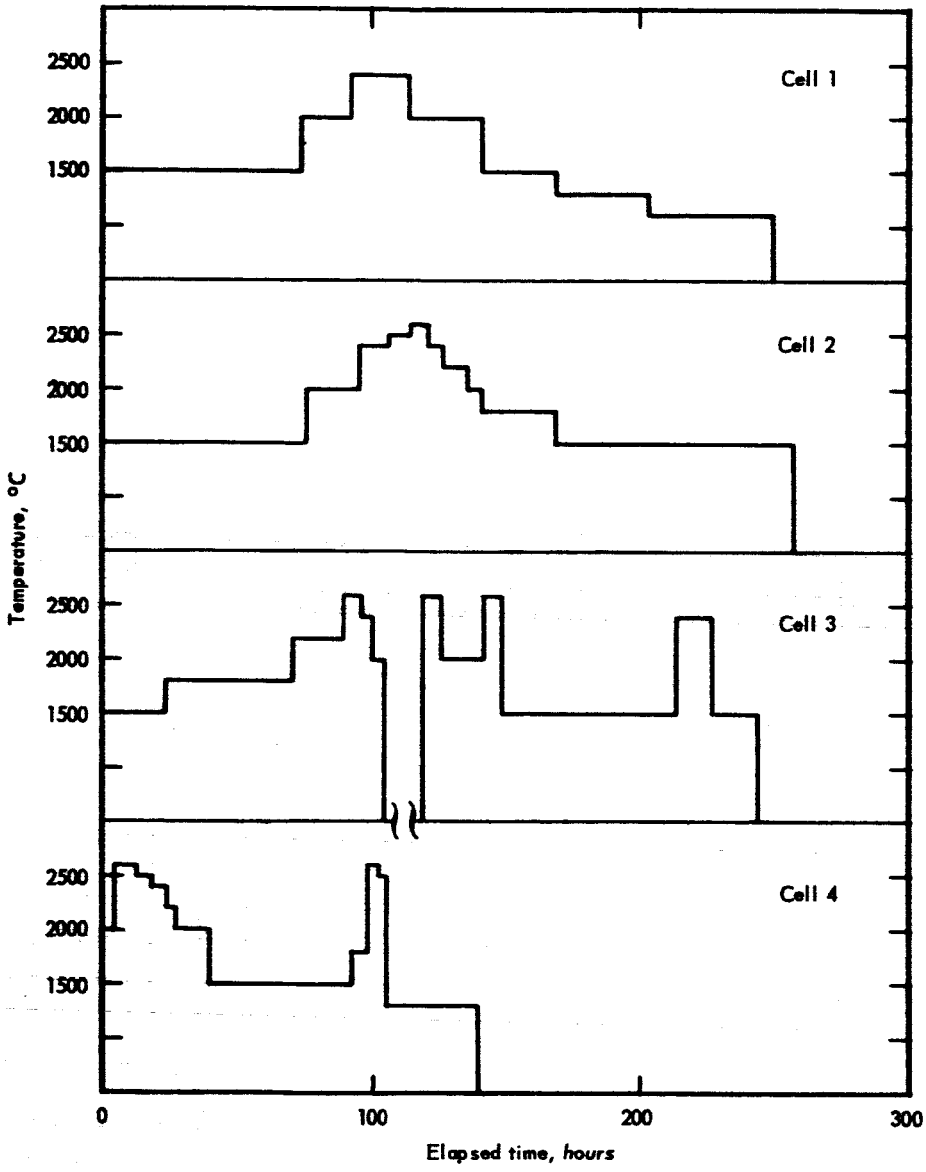

Fig. 8 – Thermal histories of hydrogen permeation cells

TABLE 2

PERMEATION COEFFICIENTS FOR HYDROGEN THROUGH ARC-CAST TUNGSTEN

Temperature, °C[a]	Hydrogen Permeation Coefficient[b]					
	Cell 2		Cell 3		Cell 4	
	1 atm	0.1 atm	1 atm	0.1 atm	1 atm	0.1 atm
1300					0.0013	–
1500	0.0024	0.00094	0.0030	–	0.0033	0.0031
1500	0.0023	–	0.0033	–		
1500			0.0032	–		
1540	0.0032	0.0038				
1800			0.012	–	0.010	–
1840	0.011	0.010				
2000	0.021	0.022	0.023	–	0.023	–
2000			0.025	–	0.021	0.021
2000			0.025	–		
2040	0.024	–				
2200			0.043	0.041	0.033	–
2240	0.042	0.042				
2400	0.067[c]	0.071[c]	0.071	–	0.054	0.052
2400			0.066	–		
2440	0.070	–				
2500	0.088[c]	0.086[c]	0.086	–	0.064	0.063
2500					0.071	–
2600	0.11[c]	0.11[c]	0.11	0.11	0.082	0.071
2600			0.11	–	0.078	–
2600			0.11	–	0.086	0.078

[a] Probable accuracy ± 10 °C.

[b] cc (STP)-mm/cm^2-min.-atm$^{1/2}$.

[c] Temperature shown may be low by as much as 20°C as a result of fogging of the window through which measurements were made.

The logarithms of permeation coefficients are plotted versus reciprocal absolute temperature in Figure 9. Least squares analysis of the data from each of the three cells separately led to values for the activation energy of 34.5, 32.5, and 29.8 kcal for cells 2, 3, and 4, respectively. These values are probably significantly different, as indicated by a 2σ deviation of about 0.8 kcal for each. For cell 2, the 0.1 atmosphere point at 1500°C was omitted; for cell 4, the four 0.1 atmosphere points at 2400°C and above were also omitted. The line shown in Figure 9 results from a composite least squares analysis of all data except the five omissions mentioned. The activation energy is 33 kcal with a 2σ deviation of 1.0 kcal. This corresponds to an uncertainty of ± 3.0 percent at the 95 percent confidence level. The line is represented by the equation

$$P = 33.2 \exp(-33{,}000/RT)$$

with half the experimental points within 10.3 percent of the line.

This curve is compared in Figure 10 with curves extrapolated from Webb's[2] and Steigerwald's[1] lower temperature permeation data obtained using non-isothermal cylindrical membranes, although the validity of such long extrapolations is doubtful. The higher activation energy and lower permeation coefficients obtained from the present work are consistent with what one might expect from higher temperature measurements, assuming that measurements at higher temperatures are characteristic of intrinsic permeation and

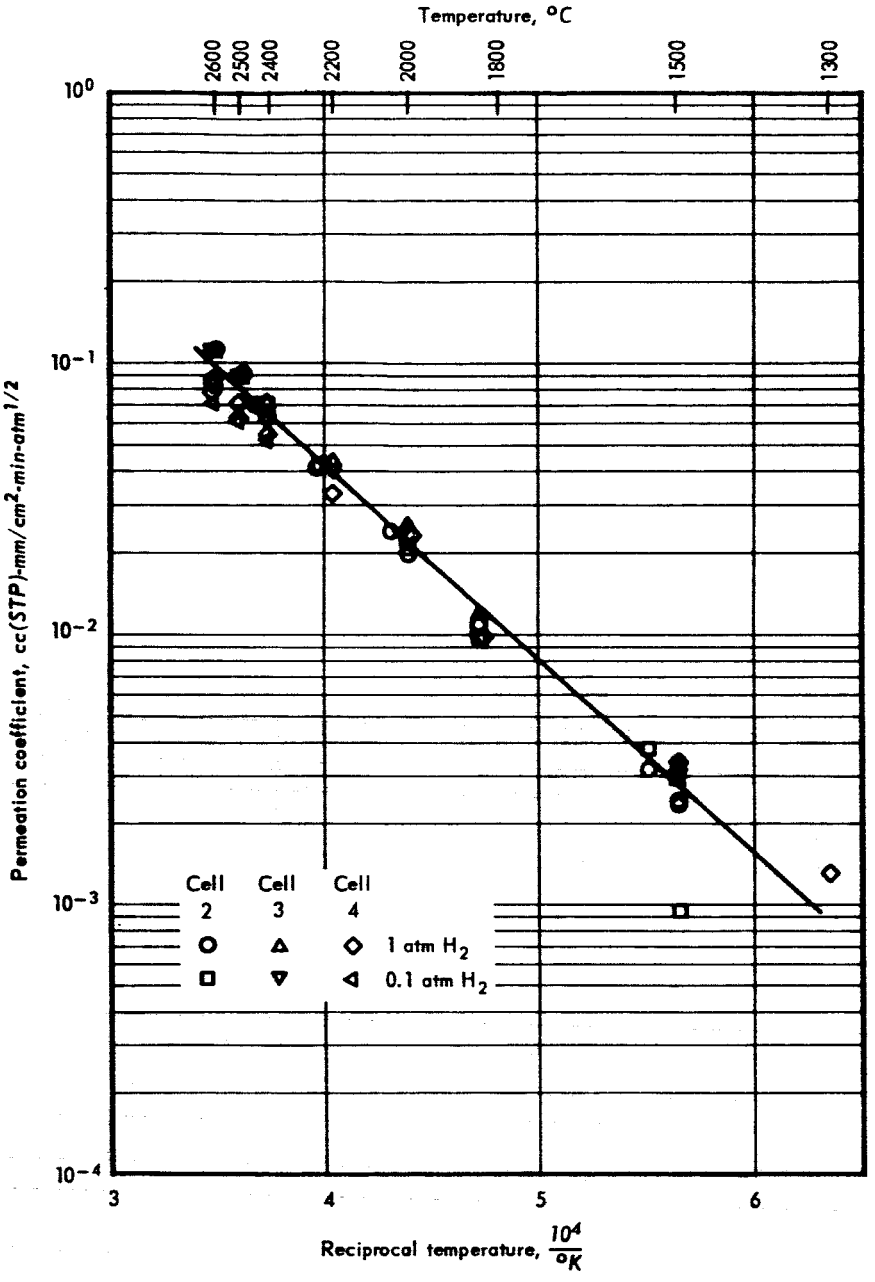

Fig. 9 – Arrhenius plot of permeation coefficients for hydrogen through arc-cast tungsten

that measurements at lower temperatures may include extrinsic effects (e. g. at lower temperatures, diffusion rates along internal surfaces are generally greater than lattice diffusion rates and have lower activation energies, hence the effect on over-all permeation rate is proportionally greater).

It is of interest to apply the present permeation data to an estimate of hydrogen solubility in tungsten, using the basic relationship:

$$P = \text{Solubility (S)} \times \text{Diffusion coefficient (D)}$$

Two studies of hydrogen diffusion in tungsten as a function of temperature have been reported.[3,4] The study by Ryabchikov is considered the more reliable on the basis of values

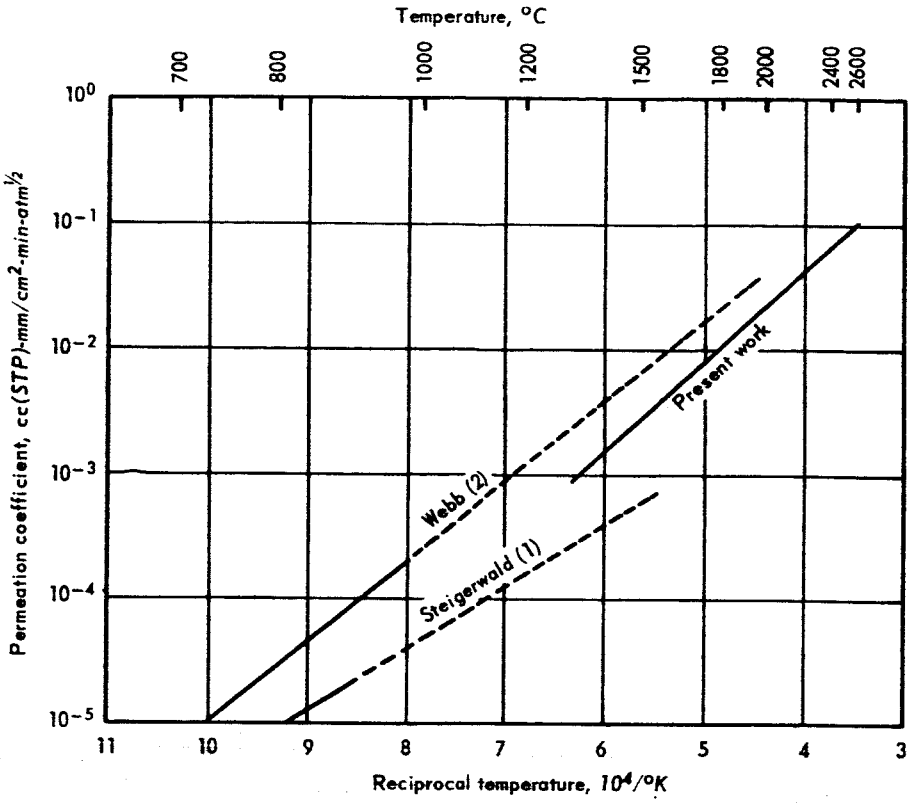

Fig. 10 – Arrhenius plot of permeation coefficients for hydrogen through arc-cast tungsten

of 0.081 for D_o and 19.8 kcal for the activation energy which he obtained from his data, and which qualitatively agree with corresponding values for hydrogen diffusion in other body-centered cubic metals. Using the data of Ryabchikov together with the permeation coefficients in Table 2, the following solubility estimates are made. These refer to the amount dissolved in equilibrium with one atmosphere of hydrogen gas.

	1700°C	2000°C	2600°C
$cc H_2(STP)/cm^3 W$	0.021	0.038	0.072
$cc H_2(STP)/gW$	0.0011	0.0020	0.0038

Tentative results from measurements of the solubility* lend support to these estimates. Similar solubility estimates based on diffusion coefficients from Moore and Unterwald[3] are about four orders of magnitude higher, and appear to be considerably suspect.

The microstructure of the membranes changed during testing from their initial fibrous structure to large equiaxed grains as shown in Figure 11. The bonding between the membrane and the arc-cast tungsten tubes to which it was electron beam welded is also shown in the figure. (The membrane shown is from cell 1 which developed a leak during testing and consequently resulted in questionable data. In subsequent cells, the inside diameters of the tubes were not mismatched as they were in this cell.) Radiographs of the cells after testing are shown in Figure 12.

Oxygen Permeation

All oxygen permeation capsules which were tested are listed in Table 3 with descriptions, test conditions, and percentage of oxygen which was lost during testing. Several

*Unpublished data obtained in this laboratory for one atmosphere hydrogen pressure.

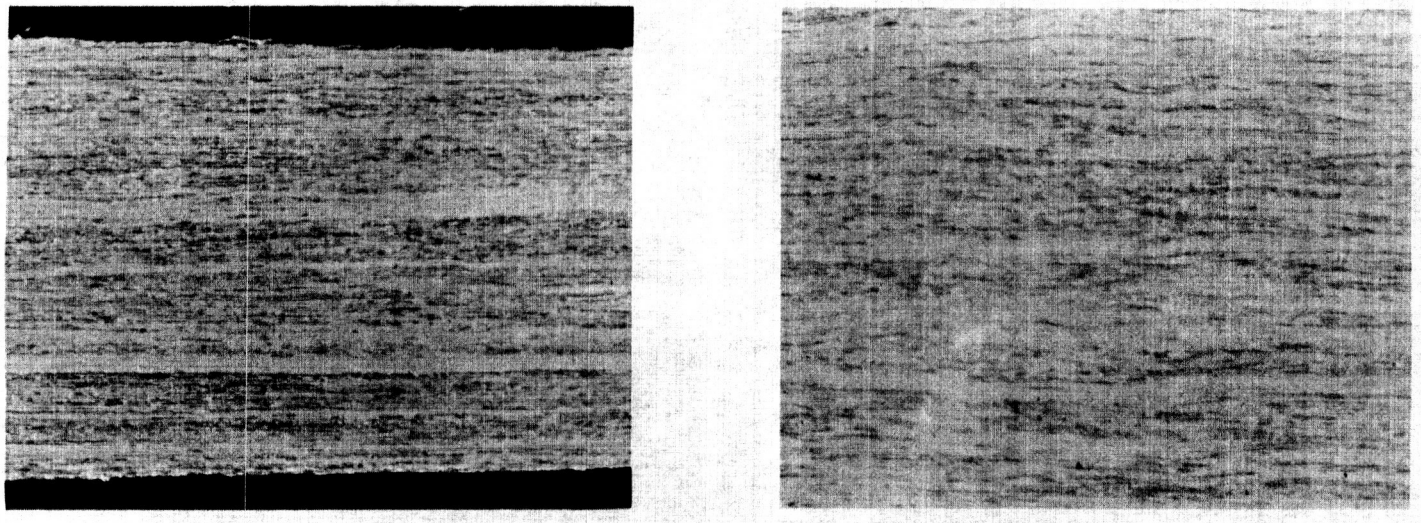

0.26 mm sheet (Neg. 6342, 20% Murakamis etchant, 250X)

0.53 mm sheet (Neg. 6341, 20% Murakamis etchant, 250X)

(a) Arc-cast tungsten membranes before testing

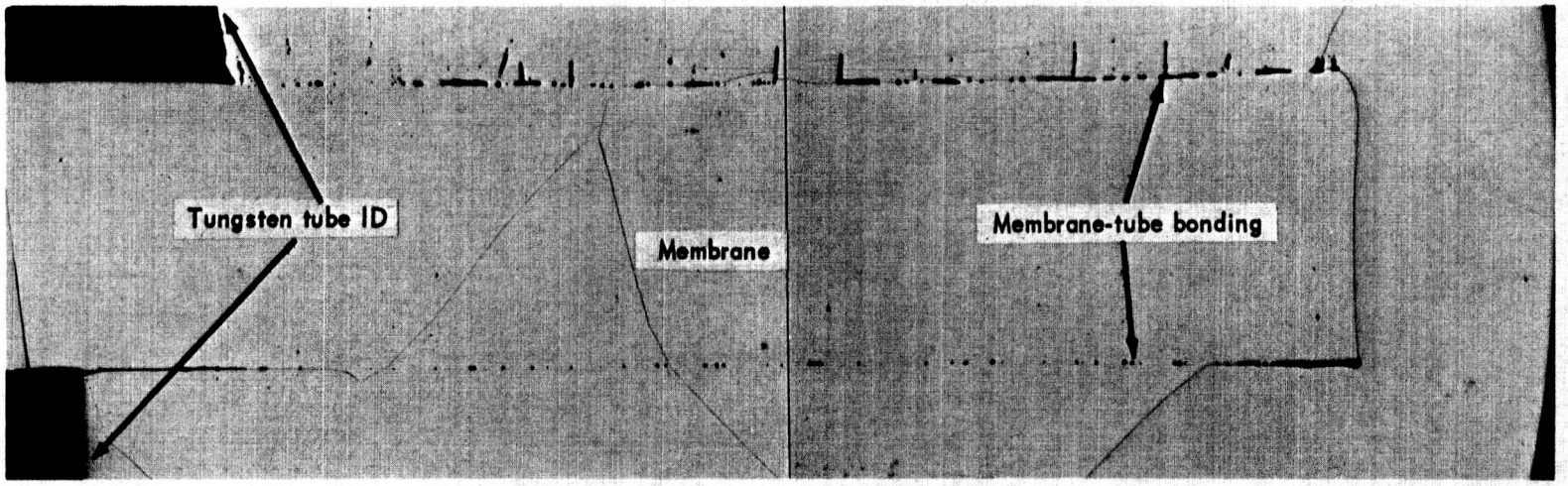

(Neg. 6893 and 6953, 20% Murakamis etchant, 75X)

(b) Arc-cast tungsten membrane electron beam welded to two arc-cast tungsten tubes. Tested 249 hours including 50 hours at temperatures exceeding 1500°C. (Cell No. 1)

Fig. 11 – Microstructure of arc-cast tungsten/hydrogen permeation cell membrane before and after testing, showing change from initial fibraus structure (a) to large equiaxed grains (b)

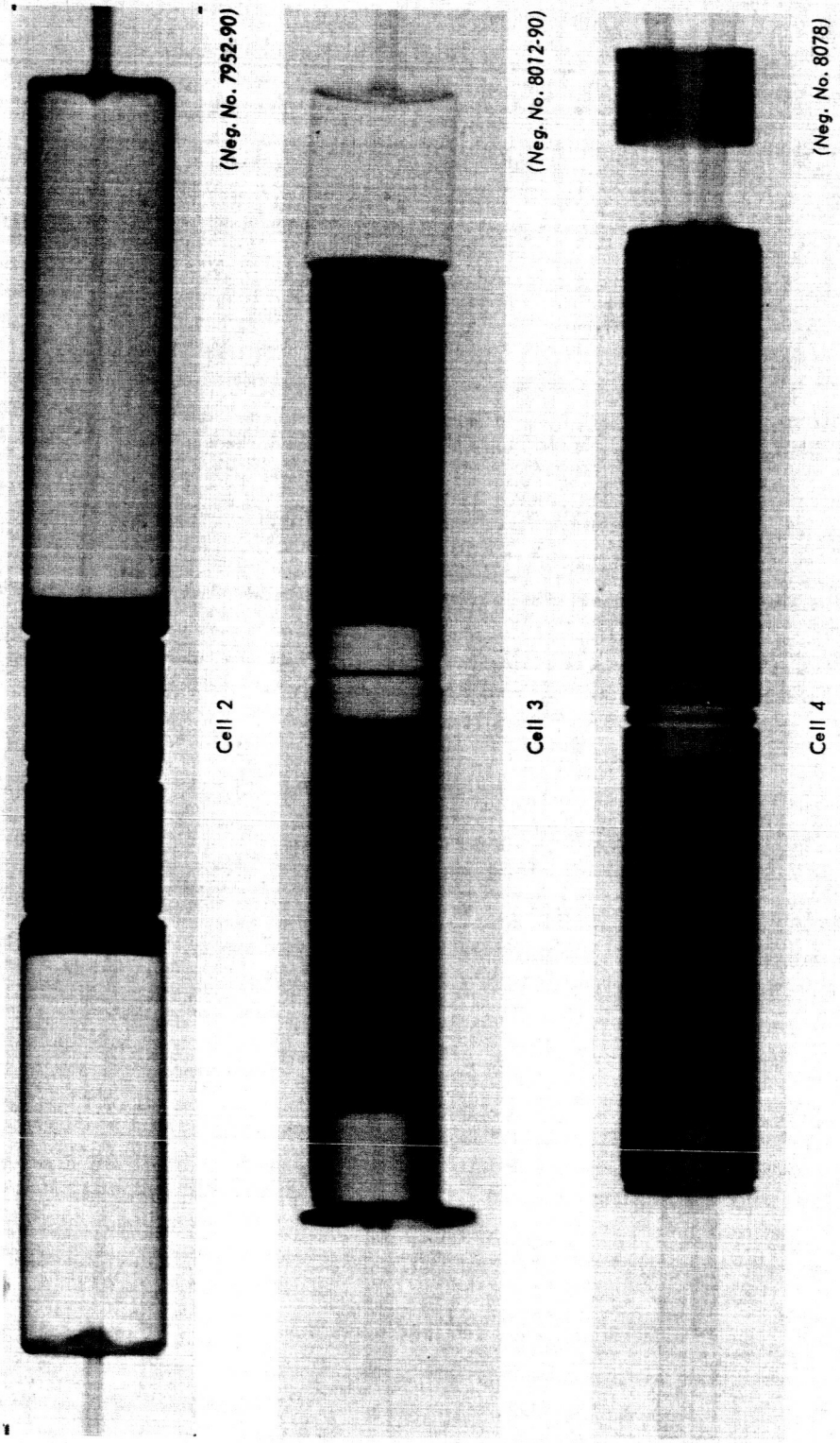

Fig. 12 – Radiographs of hydrogen permeation cells

TABLE 3

OXYGEN/TUNGSTEN PERMEATION EXPERIMENTS

Specimen No.	Type	Avg Wall Thickness, mm	Average Surface Area, cm^2	Quantity WO_3, mg	WO_3/vol, mg/cc	Time, hr	Temperature, °C	Atm.	Oxygen Lost % ± 3.5	Remarks[a]
O-2	Arc-cast	3.30	16.8	28.9	10.1	100	2600	He	~100	No residual gas – No reducible oxide
O-3	Arc-cast	3.03	16.6	29.4	10.2	100	2600	H_2	~0 (?)	~4 mm ΔP (~90% H_2 / ~10% Air); ~7 mg H_2O – No reducible oxide
O-101	Powder met. (95% T. D.)	1.20	14.8	34.6	10.2	1	2600	He	~100	Residual gas (if any) not collected – No reducible oxide
O-103	Powder met. (95% T. D.)	1.27	14.6	96.9	29.8	1	1500	He	4.0	~25μ ΔP (air); reddish purple crystals on top, brownish gold surface adjacent to top
O-104	Powder met. (95% T. D.)	1.18	14.8	96.4	29.1	1	2000	He	3.2	~2 mm ΔP (mostly He); reddish purple on top, brownish gold on sides adjacent to top
O-11	Arc-cast	0.51	10.6	60.7	28.1	5	2100	He	51.8	~5μ ΔP; reddish purple top, gold material (molten looking) on side
O-201	Arc-cast ends Electro-deposited walls	0.42	10.2	79.2	35.2	5	2100	He	(Leaked)	Small hole through side after test – No oxide remained
O-202	Arc-cast ends Electro-deposited walls	0.42	10.3	80.4	35.3	5	2100	He	77.0	Broke prematurely – Residual gas (if any) lost – reddish purple top
O-203	Arc-cast ends Electro-deposited walls	0.42	10.1	67.1	30.2	1	2400	He	(Leaked)	Small hole through side after test – No oxide remained
O-204	Arc-cast ends Electro-deposited walls	0.42	10.3	69.7	30.5	1	2400	He	(Leaked)	Small hole through side after test – No oxide remained
O-205	Arc-cast ends Electro-deposited walls	0.42	10.0	70.6	32.2	2	2100	He	31.0	~30μ ΔP; reddish purple crystals on top and adjacent side, brownish gold material on side wall
O-206	Arc-cast ends Electro-deposited walls	0.42	10.3	31.0	13.6	1-1/4	2400	He	(Leaked)	Small hole through wall at one end – No oxide remained
O-207	Arc-cast ends Electro-deposited walls	0.42	10.3	69.9	30.5	3-1/2	2100	He	(Leaked)	Small hole through wall ~1/6 way from one end – No oxide remaining
O-105	Powder met. (95% T. D.)	1.29	15.0	100.7	30.0	3	2100	He	13.0	Small hole ~1/8 way from bottom end – some reddish brown and brownish gold oxide left
O-106	Powder met. (95% T. D.)	1.43	15.0	99.9	30.4	2-1/2	2100	He	9.0	~20μ ΔP; gold material on top and walls adjacent to top, small patch purple material in center of top

TABLE 3 (Cont.)

OXYGEN/TUNGSTEN PERMEATION EXPERIMENTS

Specimen No.	Type	Avg Wall Thickness, mm	Average Surface Area, cm^2	Quantity WO_3, mg	WO_3/vol, mg/cc	Time, hr	Temperature, °C	Atm.	Oxygen Lost % ± 3.5	Remarks[a]
O-4	Arc-cast	3.02	16.8	100.5	34.1	100	2600	H_2	~100	2 mm ΔP (H_2); no water – No reducible oxide
O-1	P-M sheet ends Vapor deposited walls	0.76	9.27	16.1	10.1	5	2100	He	~100	~25μ ΔP; no reducible oxide
O-15	Arc-cast	0.51	11.2	68.6	29.6	5	2100	H_2	35.0	~3 mm ΔP (H_2); one patch of purple on one end – brownish gold material on top, bottom and side walls
O-108	Powder met. (99% T. D.)	1.21	15.2	100.1	28.6	6	2100	He	21.0	~0 ΔP; purple material on top
O-208	Arc-cast ends Electro-deposited walls	0.45	10.4	69.5	30.2	5	2000	He	15.1	~120μ ΔP; purple material on top
O-209	Arc-cast ends Electro-deposited walls	0.45	10.8	69.0	28.5	3-1/2	2100	He	(Leaked)	No oxide remaining
O-107	Powder met. (99% T. D.)	1.34	14.9	100.4	30.1	1	2300	He	16.2	~6μ ΔP; purple on top – gold along side
O-12	Arc-cast	0.52	8.45	62.3	38.9	1	2200	He	38.6	Very small ΔP; purple material on top and side walls
O-16	Arc-cast	0.51	11.2	69.0	29.7	2	2200	He	30.8	~180μ ΔP; ($\begin{matrix}Air\\CO_2\\CO\end{matrix}$); purple on top and ~1/8 inch down sides; gold adj. to purple on sides
O-109	Powder met. (99% T. D.)	1.19	15.1	100.4	29.1	1	2300	He	16.7	~13μ ΔP; purple on top and adj. walls; spot of gold on top
O-212	Arc-cast ends Electro-deposited walls	0.45	10.5	70.7	30.6	3-1/2	2150	He	No analysis	~15μ ΔP; most of top gold color; small area of purple in center of top
O-50	Arc-cast	2.55	15.7	92.6	31.0	1	2300	He	14.6	~45μ ΔP; reddish purple crystals inside top
O-51	Arc-cast	2.55	15.6	94.5	32.0	4	2200	He	14.8	~80μ ΔP; reddish purple crystals inside top
O-17	Arc-cast	0.51	10.7	69.0	31.8	16	1985	He	37.0	~0μ ΔP; reddish purple and golden crystals
O-53	Arc-cast	2.55	15.3	101.6	34.8	3	2300+	He	19.0	~200μ ΔP; reddish purple and golden crystals
O-54	Arc-cast	2.55	15.5	102.9	31.1	11.5	2200	He	51.2	~1 mm ΔP; reddish purple and golden crystals

[a]Pressure in specimen estimated to be ~30 times pressure rise of apparatus.

capsules developed leaks during testing. The leak-free capsules are listed in Table 4 with their test conditions and calculated permeation coefficients for oxygen through tungsten. A sample permeation coefficient calculation is shown in Appendix C.

TABLE 4

SUMMARY OF OXYGEN/TUNGSTEN PERMEATION EXPERIMENTS

Test Temperature, °C	Specimen No.	Type[a]	Time, hr	Atmosphere	Oxygen Lost % ± 3.5	Avg O_2 Press Atmosphere	Permeation Coefficient[b]
2600	O-101	P-M(95%TD)	1	He	~100	9.4×10^{-4}	>0.22
	O-2	A-C	100	He	~100	9.4×10^{-4}	>0.0043
	O-3	A-C	100	H_2	~0		
	O-4	A-C	100	H_2	~100	1.3×10^{-3}	>0.012
2300	O-107	P-M(99%TD)	1	He	16.2	3.2×10^{-4}	0.20
	O-109	P-M(99%TD)	1	He	16.7	3.2×10^{-4}	0.18
	O-50	A-C	1	He	14.6	3.2×10^{-4}	0.29
	O-53	A-C	3	He	19.0	3.3×10^{-4}	0.14
2200	O-12	A-C	1	He	38.6	1.5×10^{-4}	0.29
	O-16	A-C	2	He	30.8	1.3×10^{-4}	0.10
	O-51	A-C	4	He	14.8	1.4×10^{-4}	0.11
	O-54	A-C	11.5	He	51.2	1.4×10^{-4}	0.15
2100	O-205	E-D	2	He	31.0	5.8×10^{-5}	0.15
	O-106	P-M(95%TD)	2.5	He	9.0	5.9×10^{-5}	0.11
	O-105	P-M(95%TD)	3	He	12.0	5.9×10^{-5}	0.11
	O-11	A-C	5	He	51.8	5.4×10^{-5}	0.10
	O-202	E-D	5	He	77.0	5.2×10^{-5}	0.17
	O-1	V-D	5	He	~100	2.3×10^{-5}	>0.15
	O-15	A-C	5	H_2	35.0	5.7×10^{-5}	0.071
	O-108	P-M(99%TD)	6	He	21.0	5.7×10^{-5}	0.089
2000	O-104	P-M(95%TD)	1	He	3.2	2.2×10^{-5}	0.13
	O-208	E-D	5	He	15.1	2.2×10^{-5}	0.047
1965	O-17	A-C	16	He	37.0	2.2×10^{-5}	0.040

[a] P-M = powder metallurgy; A-C = Arc-cast; E-D = electro-deposited; V-D = vapor deposited.
[b] For oxygen (O_2) through tungsten; cc (STP)-mm/cm^2-min-atm$^{1/2}$.

Oxygen loss from the capsules appears to be linear with time as shown in Figure 13, although the 1-hour data point appears to show too high a loss rate. In the figure, quantity of permeated gas, normalized to unit thickness, surface area, and pressure is plotted versus time for specimens of like material which were tested at a given temperature. The data also indicate that the quantity of oxygen lost is a function of wall thickness (i. e., at 2200°C, the 0.51 mm wall capsule lost ~30% in 2 hours and the 2.55 mm wall capsule lost ~50% in 11.5 hours) suggesting that diffusion is the rate controlling step.

In each instance where oxide remained after testing, it was present as reddish purple crystals condensed on the interior surface of the top of the capsule, or brownish gold material which was present at the same location or on the sidewalls adjacent to the top. After reduction, wall fragments of a few capsules were analyzed for oxygen content to assure that the oxygen which was accounted for as lost from the capsules was not partly dissolved in the specimen walls. Fragments taken from different parts of specimen O-2, heated at 2600°C for 100 hours (100% oxygen loss), showed oxygen contents of less than 10 ppm (7 determinations ranged from 1. 5 to 9. 4 ppm). Specimen O-11 heated 5 hours at 2100°C (~50% oxygen loss) had an oxygen content of 4 ppm.

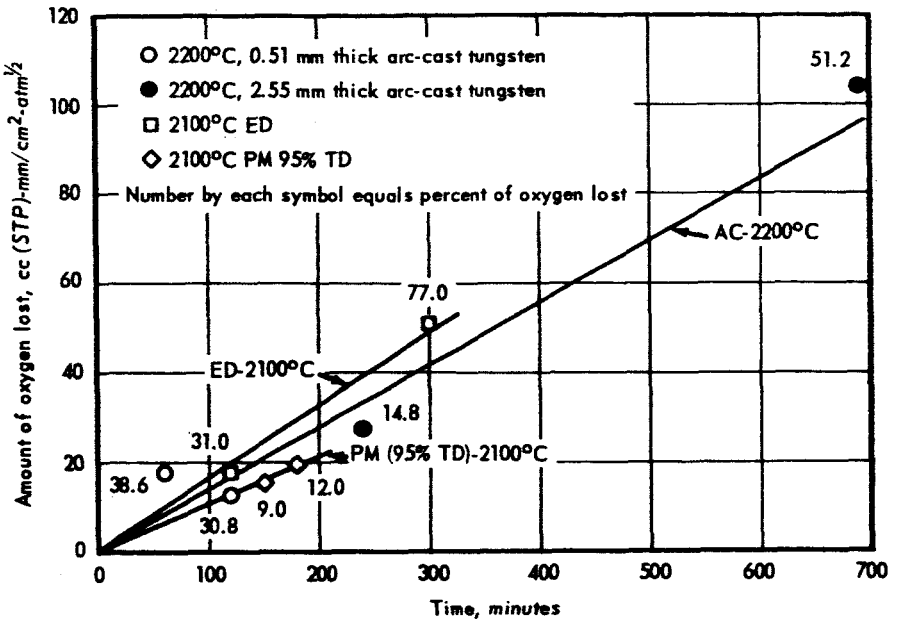

Fig. 13 – Oxygen loss versus time for capsules tested at the same temperature

The logarithms of permeation coefficients are plotted versus reciprocal of absolute temperature in Figure 14. A line representing a least squares fit to all of the data has a slope corresponding to an activation energy of about 40 kcal/mole. A separate line representing a least squares fit to the coefficients obtained from arc-cast specimens, omitting the two 1-hour runs, has a slope which corresponds to an activation energy of about 44 kcal/mole. Equations describing these lines are:

$$P = 850 \exp(-44{,}000 \pm 9{,}000/RT) \text{ for arc-cast tungsten,}$$

and

$$P = 510 \exp(-40{,}000 \pm 10{,}000/RT) \text{ for all types.}$$

The $\pm$ factor is the 2σ deviation from a least squares fit of the data.

The large uncertainty in these activation energies is a result of the factor of three spread in the data, which may indicate that in at least some of the tests, some oxygen loss occurred by a non-diffusion process. That is, the average permeation coefficients at each temperature may be somewhat high. Other possible causes of data scatter are: (1) several different types of tungsten were used (arc-cast, powder metallurgy – two densities –, and electro-deposited), (2) each permeation coefficient was obtained from a separate specimen, and (3) an unknown error exists in the actual time at temperature for short (~1 hour) test times at the higher temperatures in that heating and cooling times were a significant fraction of test time.

In addition to the scatter in the oxygen permeation coefficients, they are higher than corresponding hydrogen permeation coefficients. This unexpected result raises a question as to the possibility of a consistent bias in the oxygen permeation coefficients. It is believed that the only potentially significant source of bias is in the assignment of values for the oxygen partial pressure on the two sides of the capsule wall: (1) on the inside of the capsule, the partial pressure is calculated as described in Appendix B, and (2) on the outside, it is assumed to be zero.

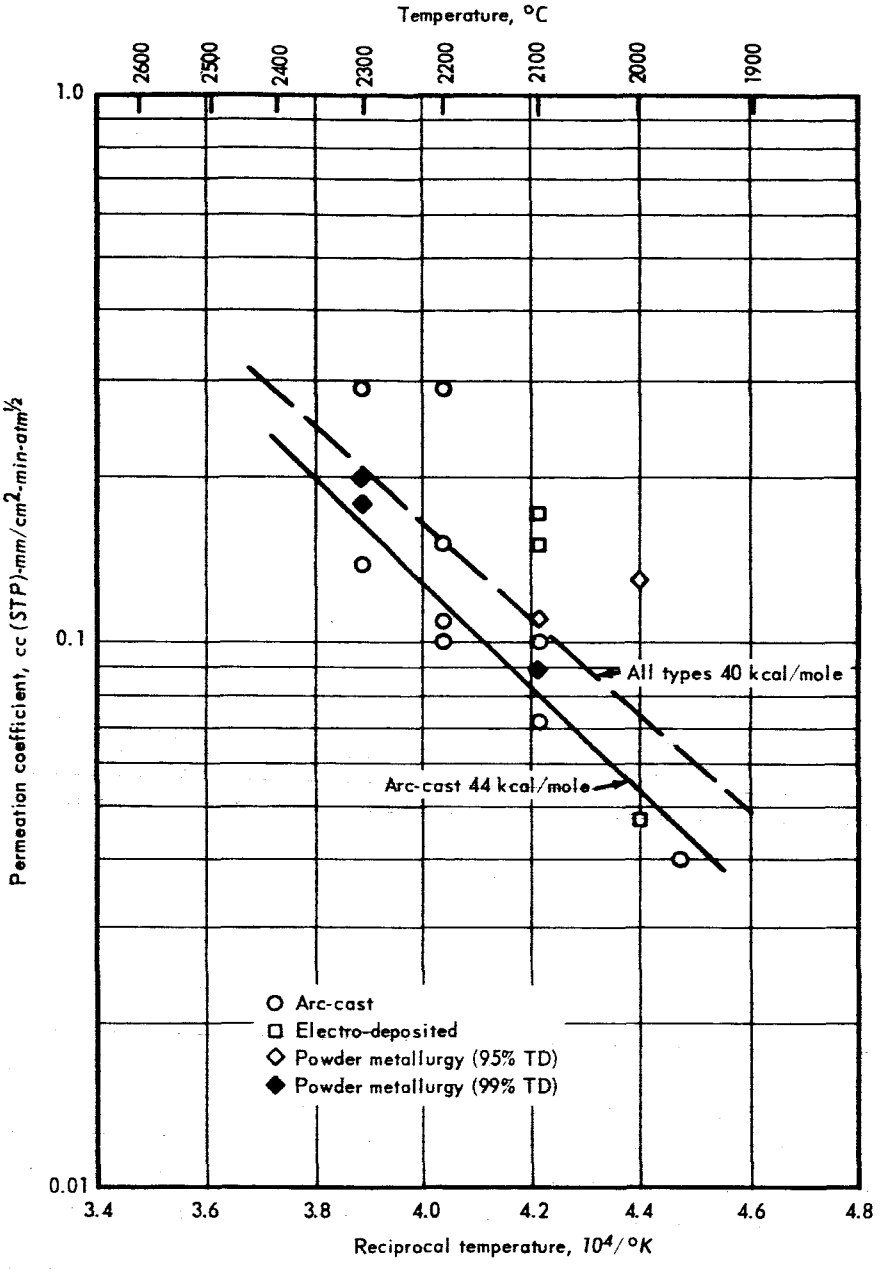

Fig. 14 – Arrhenius plot of permeation coefficients for oxygen through tungsten

In the first instance, values of the permeation coefficients are entirely dependent on the accuracy of the calculations for oxygen pressure inside the capsule as given in Appendix B. In making these calculations, it was assumed that the enthalpy and entropy values obtained in the 1000° to 1200°C range were constant with temperature and thus the ΔF was linear with temperature. In order to assess this source of bias, 5 and 10 percent errors in the enthalpy and entropy values were assigned such that the net effect was to raise the calculated oxygen partial pressure in the capsule, thereby lowering the permeation coefficient. It is believed that these errors introduce a sufficiently large bias to include conservatively the uncertainties in both the original enthalpy and entropy values and the extrapolation to test temperatures. These errors reduced the calculated permeation coefficients by factors of 2 and 5, respectively. A factor of 5 bias in the direc-

tion of lower permeation coefficients is thus believed larger than actually exists in the present permeation coefficients.

In the second instance, if the assumption that the partial pressure of oxygen outside the capsule is zero is incorrect, the calculated permeation coefficients are too low. That the oxygen pressure outside the capsule is significantly above zero is very unlikely, since any oxygen in the sweep gas, including that which permeated the capsule, would be present largely as W_xO_y. The oxygen partial pressure would be that in equilibrium with W_xO_y (at a low total pressure) and should not significantly increase the total oxygen pressure outside the capsule.

The validity of the permeation rates can also be assessed by estimating oxygen diffusion coefficients in tungsten, using the relationship that permeation is equal to the product of diffusion and solubility, and comparing these D values with D values for oxygen in tungsten from the literature. The only solubility value in the literature is for 1700°C, reported by Allen, et al.,[8] which was obtained from tungsten rods annealed with excess WO_3 in sealed capsules. The oxygen partial pressure in equilibrium with the measured solubility of 40 ppm (0.54 cc(STP)/cm^3 of W) was not reported, but a value of 7×10^{-7} atmospheres was obtained for this pressure assuming experimental conditions and using computations similar to those given in Appendix B. Permeation rates under the same pressure conditions were obtained by extrapolation of the curves in Figure 14 with suitable pressure conversions, and were combined with this solubility value to give diffusion coefficients. These diffusion coefficients are shown in Table 5 together with diffusion coefficients from the literature for oxygen in tungsten.[5-8] The diffusion coefficients deduced from the present work are within the range of values reported in the literature for oxygen in tungsten. These diffusion coefficients are also in the range of values (1×10^{-10} to 7×10^{-6}) obtained for the diffusion of oxygen, nitrogen, and carbon in tungsten, niobium, and tantalum for the same homologous temperature.[12-23]

TABLE 5

DIFFUSION COEFFICIENTS FOR OXYGEN IN TUNGSTEN AT 0.536 TIMES THE MELTING POINT (1700°C)

Source	Diffusion Coefficient, cm^2/sec
ref 7, 8	1×10^{-7}
ref 5	2.9×10^{-3}
ref 6	1.3×10^{-9}
GE-NMPO (40 ± 10 kcal curve)[a]	5×10^{-8} (4×10^{-9} to 6×10^{-7})[b]
GE-NMPO (44 ± 9 kcal curve)[a]	3×10^{-8} (3×10^{-9} to 3×10^{-7})[b]

[a]Calculated from equation: D = P/S.

[b]Range of the calculated D using the 2σ deviation indicated for the activation energies.

Considering the possible sources of error and estimated diffusion coefficients, the observed oxygen permeation coefficients are believed to be of the right magnitude.

The microstructures of the tubing from which capsules were fabricated, and microstructures of some of the capsules after testing are shown in Figures 15 and 16. The expected change in microstructure from the worked to recrystallized structure is quite evident.

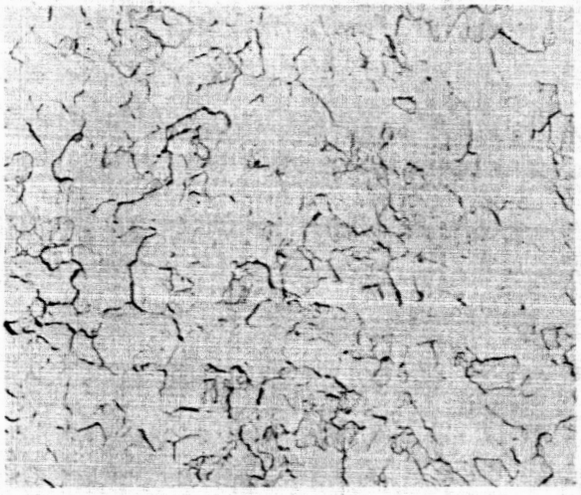

(Neg. 6343, 20% Murakamis etchant, 250X)

As-received

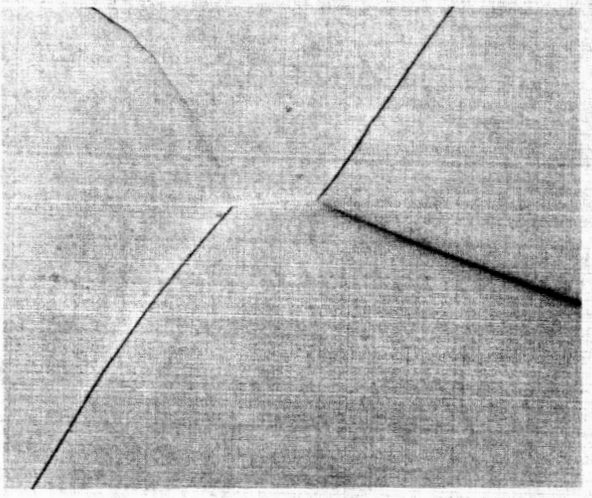

(Neg. 6946, 20% Murakamis etchant, 100X)

Tested 100 hours at 2600°C in He

(a) Arc-cast tungsten tubing, 1.9 cm OD x 2.5 mm wall

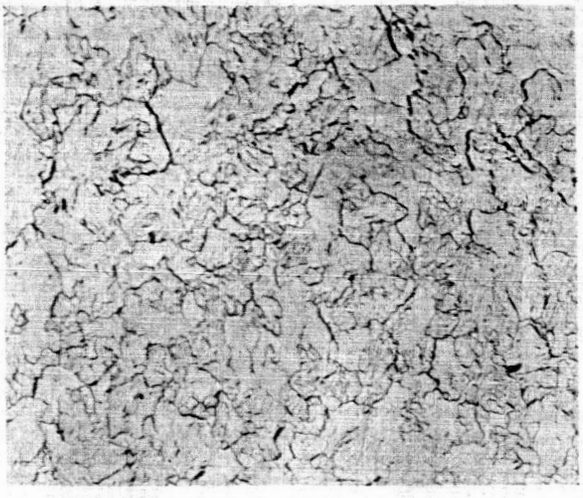

(Neg. 6344, 20% Murakamis etchant, 250X)

As-received

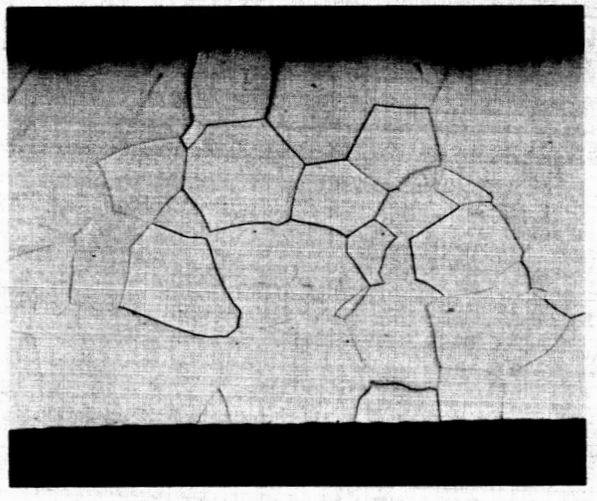

(Neg. 7088, 20% Murakamis etchant, 100X)

Tested 1 hour at 2200°C in He

(b) Arc-cast tungsten tubing, 1.2 cm OD x 0.52 mm wall

Fig. 15 – Microstructures of arc-cast tungsten/oxygen permeation capsules before and after testing

Comparison of Hydrogen and Oxygen Permeation Rates

As already indicated, observed oxygen permeation coefficients are higher (2 to 5 times) than hydrogen permeation coefficients. Recalling the solubility data cited earlier, the higher permeation coefficients for oxygen are attributed to a much higher solubility. At 1700°C, the solubility of oxygen is 0.54 cc(STP)/cm^3 at an assumed oxygen partial pressure (P_{O_2}) of 7×10^{-7} atmospheres, and the solubility of hydrogen is estimated as 0.021 cc(STP)/cm^3 for one atmosphere of hydrogen pressure. If the latter is adjusted to a partial pressure (P_{H_2}) of 7×10^{-7}, it is apparent that oxygen solubility is greater than hydro-

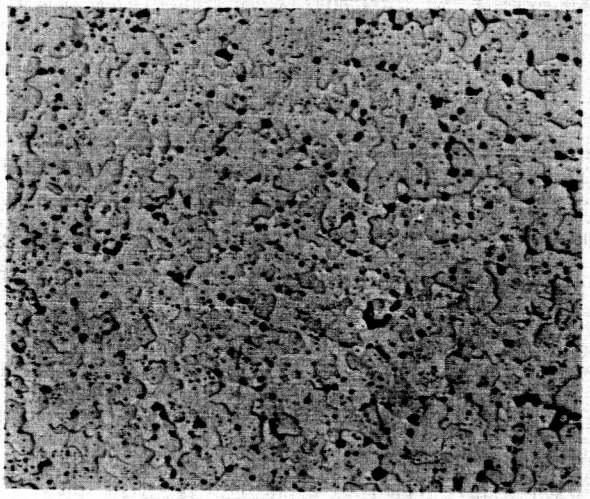

(Neg. 6948, 20% Murakamis etchant, 100X)

95% theoretical density

Tested 1 hour at 2000°C in He

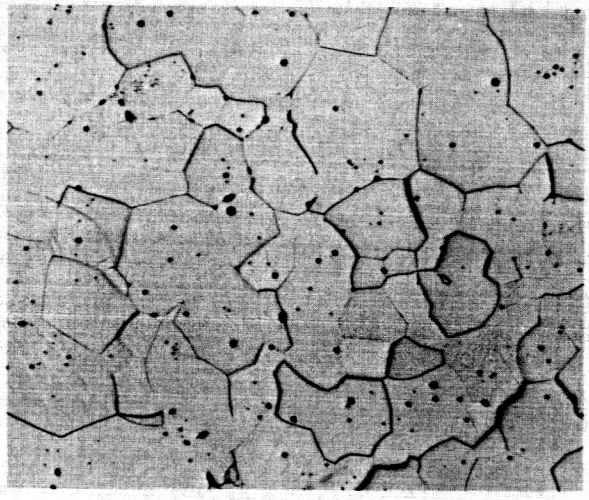

(Neg. 6949, 20% Murakamis etchant, 100X)

99% theoretical density

Tested 1 hour at 2300°C in He

(a) Fabricated by powder metallurgy techniques

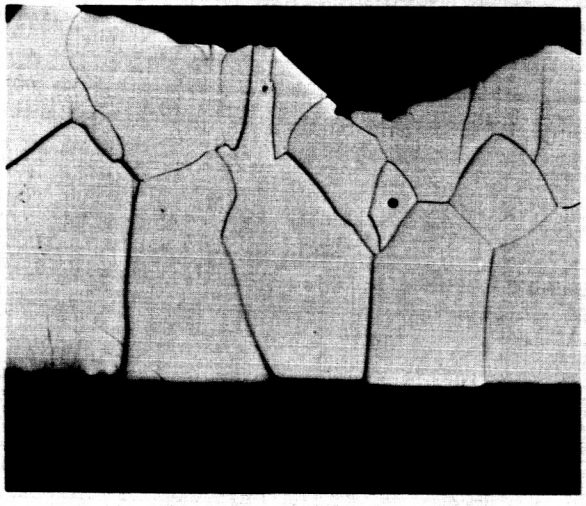

(Neg. 6950, 20% Murakamis etchant, 100X)

Tested 5 hours at 2100°C in He

(b) Fabricated from electro-deposited tungsten

Fig. 16 – Microstructures of oxygen permeation capsules after testing

gen solubility by a factor considerably greater than indicated by the ratio 0.54/0.02. This adjustment cannot be reliably calculated since the exact relationship between solubility and pressure over such a wide range is not known.

If both the solubilities and permeation coefficients are essentially correct, oxygen diffusion is about 4 decades lower than hydrogen diffusion in tungsten at 1700°C. This is in good agreement with similar data for niobium where oxygen diffusion is 2 to 3 decades lower than hydrogen diffusion at the same homologous temperature (1170°C).[4,12,13,24] These comparisons offer additional evidence that the oxygen permeation coefficients are valid

within a decade and in the temperature range considered here are similar in magnitude to the hydrogen permeation coefficients.

CONCLUSIONS AND RECOMMENDATIONS

Permeation coefficients were determined experimentally for hydrogen permeation through arc-cast tungsten in the temperature range 1300° to 2600°C. Permeation rates were very nearly proportional to the difference between the square roots of hydrogen pressure on each side of the membrane and inversely proportional to membrane thickness, indicating that atomic hydrogen is the diffusing species. Permeation coefficients were dependent on absolute temperature according to the equation:

$$P = 33.2 \exp(-33{,}000/RT) \text{ with a } 2\sigma \text{ limit of } \pm 1000 \text{ cal in the activation energy.}$$

Permeation rates of oxygen through tungsten were determined using sealed capsules containing known quantities of tungsten oxide. Permeation coefficients for oxygen were higher than those for hydrogen in the temperature range studied. This is probably the result of oxygen solubility being much greater than hydrogen solubility at these temperatures. The activation energy for oxygen permeation through tungsten is probably higher than that for hydrogen permeation.

Additional oxygen permeation experiments, using arc-cast tungsten of different wall thicknesses, should be performed over a wider temperature range with variable flow rates of gas past the capsule. Also, measurements of the solubility of oxygen in tungsten would help to verify the magnitude of oxygen permeation coefficients.

ACKNOWLEDGMENTS

The authors are indebted to H. C. Brassfield for his advice, counsel, and experimental assistance during the course of this work; to J. C. Yungbluth and H. G. Smith for electron beam welding; to C. E. North for TIG welding; to T. M. Welch and C. R. Muncy for experimental assistance; to A. F. Rosenberg for the determination of residual gases in the oxygen permeation capsules and to P. F. Elliot for the determination of hydrogen in the furnace sweep gas.

APPENDIX A
Materials

TUNGSTEN

The tungsten materials used in this investigation were greater than 99.9 percent tungsten.

Results of impurity analyses are given in Table A1. Data pertaining to electrodeposited material are from an analysis of the finished tubing. Data tabulated for the vacuum arc-cast tungsten represent analyses of the heats from which rod, tubing, and sheet were fabricated; the impurity contents of the rod, tubing, and sheet may be somewhat different from these values.

These data show that the interstitial impurities ranged from <1 to 50 ppm of carbon, 7 to 35 ppm oxygen, less than 15 ppm nitrogen, and undetectable quantities of hydrogen. Previous high temperature studies of arc-cast tungsten have shown that thermal treatment similar to that which the hydrogen permeation cells experienced reduces the carbon content from starting levels of 50 to 60 ppm to about 30 ppm. While molybdenum content was probably not affected by thermal treatment, the iron and nickel contents were most probably lowered.

ARGON

The argon gas used in this investigation contained about 8 ppm nitrogen. None of the following gases were present in detectable quantities (<4 ppm): hydrogen, methane, oxygen, carbon monoxide, carbon dioxide, and helium.

HYDROGEN

The major impurity in the hydrogen used was nitrogen which is normally present in quantities of about 300 ppm. Oxygen content was <50 ppm and other gases were less than 10 ppm each.

HELIUM

The nitrogen content of the helium gas was <10 ppm, oxygen <4 ppm, and methane, carbon monoxide, and carbon dioxide <1 ppm.

TABLE A1

IMPURITY ANALYSES OF TUNGSTEN

	Arc-Cast[a]						Electro-Deposited[h]
	19 mm Dia. Rod[b]	19 mm OD x 2.5 mm Wall Tubing[c]	13 mm OD x 0.51 mm Wall Tubing[d]	2.5 mm Thick Sheet[e]	0.53 mm Thick Sheet[f]	0.26 mm Thick Sheet[g]	13 mm ID x 0.37 mm Wall Tubing
C	45	40	<10	50	39	39	<1
Si	<20	<20	<20	<20	<20	<20	<1
Ti	<1	<1	<1				<1
Mn				<10			
Cr				<10			<1
Cu							90
Ni	2	1	<1		8	8	70
Mo	32	51	25				200
Fe	16	20	8	13	8	8	
O	16	35	8				7
N	3	3	13				
H	<1	<1	<1				

[a]Vendor's analysis of heats from which above materials were obtained; values in ppm.
[b]Used in fabrication of H_2 permeation cells 3 and 4 and some O_2 permeation capsules.
[c]Used in fabrication of H_2 permeation cells 1 and 2 and some O_2 permeation capsules.
[d]Used in fabrication of some O_2 permeation capsules.
[e]End caps in some O_2 permeation capsules.
[f]Membranes in H_2 permeation cells 1 and 3 and end caps of some O_2 permeation capsules.
[g]Membranes in H_2 permeation cells 2 and 4.
[h]Analysis of tubing; tubing used for O_2 permeation capsules.

APPENDIX B
Calculation of Oxygen Partial Pressure in Equilibrium with $W_x O_y$

Tungsten forms a number of oxides with complex stoichiometries, many of which are quite stable as gaseous species at high temperatures. Thus, a tungsten membrane exposed to flowing gases containing oxygen will erode and the long-term life of the membrane will be impossible to maintain. At the other extreme, a small amount of gaseous oxygen confined in a sealed tungsten capsule will be depleted as a function of the amount which permeates (assuming no interaction to form gaseous oxides), and the permeation rate will decrease with time.

The most suitable method for measuring oxygen permeation is therefore to seal a known amount of WO_3 inside a tungsten capsule. Thus, during heating, there is on the one hand no large excess of gaseous oxygen to cause erosion, yet the added tungsten oxide provides a continuing supply of oxygen which is depleted much more slowly than as a function of the amount which permeates and the permeation rate may not decrease measurably with time until the W_xO_y compounds disappear.

The data required for calculations of oxygen partial pressure were obtained from Ackermann, et al.,[25,27] Stull and Sinke[11] and DeMaria, et al.[26] Using free energies of formation for oxides according to equation (B1)

$$xW(s) + \frac{y}{2} O_2(g) \rightleftharpoons W_xO_y(g) \qquad \text{(B1)}$$

one can relate the partial pressure of W_xO_y to the partial pressure of oxygen according to equation (B2) where K is an equilibrium constant and dependent only on temperature.

$$K(T) = \frac{(P_{W_xO_y})}{(P_{O_2})^{y/2}} \qquad \text{(B2)}$$

Assuming that the temperature dependence of the free energy for equation (B1) can be expressed in linear form as $\Delta F_f = \Delta H_f - T\Delta S_f$, K(T) can be computed for each temperature. Table B1 lists the ΔH and ΔS values used in the calculations. Also included are ΔH and ΔS values for dissociation of molecular oxygen to atomic oxygen. The equations have been linearized to apply in the temperature range 1800° to 2900°K.

If there are n gaseous species of tungsten oxide in the container, there are n-1 relations of the type given by equation (B2). The partial pressure of oxygen can be determined with one further relation based on conservation of oxygen atoms distributed among the various gaseous oxides and free oxygen as shown by equation (B3):

$$\sum_y y\, K(T)\, P_{O_2}^{y/2} + K_O(T)\, P_{O_2}^{1/2} + 2P_{O_2} = \frac{3\,W}{\text{mol. wt.}} \frac{RT}{V} \qquad \text{(B3)}$$

TABLE B1

THERMODYNAMIC FUNCTIONS FOR THE FORMATION OF VARIOUS GASEOUS OXIDES

Species	y	ΔH_f cal/mole	ΔS_f cal/mole-deg.	Reference
W_4O_{12}	12	-655,600	-160.29	25
W_3O_9	9	-474,100	-110.26	25
W_3O_8	8	-400,900	- 90.54	25
W_2O_6	6	-272,500	- 54.98	25
WO_3	3	- 75,700	- 15.54	27
WO_2	2	+ 22,000	- 11.14	26
WO	1	+104,700	- 25.40	26
O	1	+ 61,076	+ 16.0	11

in which the capsule of volume (V) initially contains (W) grams of WO_3 solid. The range of capsule loadings used in this study is such that the WO_3 is completely converted to the gaseous state at test temperatures. Perfect gas law behavior is assumed.

With a computer program, equilibrium constants of the various gaseous oxides were calculated for temperatures between 1800° and 2600°C, as listed in Table B2. From these, partial pressures of the various species may be calculated for any given total pressure, or capsule loading. Sample calculations are given in Table B3 for 0.100 gram WO_3 contained in a volume of 10 cm^3. It is apparent that the principal species is W_3O_9 at 1800°C and W_2O_6 at 2600°C. Several other species, however, are present in comparable concentrations. For this capsule loading, molecular and atomic oxygen partial pressures are quite similar and vary from 10^{-6} to 10^{-3} atmospheres over the temperature range.

Similar calculations have been carried out for other capsule loadings and are shown graphically in Figures B1 through B5. These provide the basis for calculation of permeation coefficients obtained in this study.

TABLE B2

EQUILIBRIUM CONSTANTS FOR VARIOUS GASEOUS SPECIES ACCORDING TO EQUATION (B1)

Temp., °C	$K_{W_4O_{12}}$	$K_{W_3O_9}$	$K_{W_3O_8}$	$K_{W_2O_6}$	K_{WO_3}	K_{WO_2}	K_{WO}	K_O
1800	1.28+34	7.96+25	3.10+22	5.28+16	3.87+04	1.75-05	2.52-17	1.14-03
1900	8.39+30	3.97+23	3.51+20	2.51+15	1.66+04	2.24-05	8.11-17	2.25-03
2000	1.05+28	3.16+21	5.89+18	1.56+14	7.67+03	2.80-05	2.36-16	4.20-03
2100	2.31+25	3.79+19	1.40+17	1.23+13	3.78+03	3.44-05	6.27-16	7.42-03
2200	8.32+22	6.48+17	4.48+15	1.18+12	1.98+03	4.15-05	1.54-15	1.25-02
2300	4.65+20	1.52+16	1.88+14	1.37+11	1.09+03	4.94-05	3.53-15	2.03-02
2400	3.83+18	4.73+14	9.97+12	1.86+10	6.23+02	5.81-05	7.59-15	3.18-02
2500	4.45+16	1.89+13	6.54+11	2.93+09	3.73+02	6.75-05	1.55-14	4.81-02
2600	7.06+14	9.43+11	5.19+10	5.23+08	2.31+02	7.75-05	2.99-14	7.08-02

TABLE B3

PARTIAL PRESSURES (ATM) OF GASEOUS TUNGSTEN OXIDES AND FREE OXYGEN FOR 10 cc CAPSULE CONTAINING 0.1 g of WO_3

Temp., °C	$P_{W_4O_{12}}$	$P_{W_3O_9}$	$P_{W_3O_8}$	$P_{W_2O_6}$	P_{WO_3}	P_{WO_2}	P_{WO}	P_O	P_{O_2}	Total Pressure (atm)
1800	4.98-01	1.24+00	3.56-01	3.30-01	9.66-05	3.22-11	3.42-20	1.54-06	1.84-06	2.43
1900	3.93-01	1.27+00	4.56-01	5.44-01	2.44-04	1.34-10	1.99-19	5.52-06	6.00-06	2.66
2000	3.00-01	1.24+00	5.50-01	8.34-01	5.60-04	4.90-10	9.86-19	1.75-05	1.75-05	2.92
2100	2.19-01	1.15+00	6.25-01	1.19+00	1.18-03	1.58-09	4.25-18	5.03-05	4.60-05	3.19
2200	1.55-01	1.03+00	6.77-01	1.61+00	2.31-03	4.61-09	1.62-17	1.32-04	1.11-04	3.48
2300	1.06-01	8.91-01	6.99-01	2.07+00	4.21-03	1.22-08	5.54-17	3.19-04	2.47-04	3.77
2400	7.07-02	7.49-01	6.97-01	2.53+00	7.27-03	2.99-08	1.72-16	7.21-04	5.14-04	4.06
2500	4.63-02	6.15-01	6.72-01	2.99+00	1.19-02	6.79-08	4.90-16	1.53-03	1.01-03	4.33
2600	3.02-02	4.98-01	6.34-01	3.42+00	1.87-02	1.45-07	1.29-15	3.06-03	1.87-03	4.60

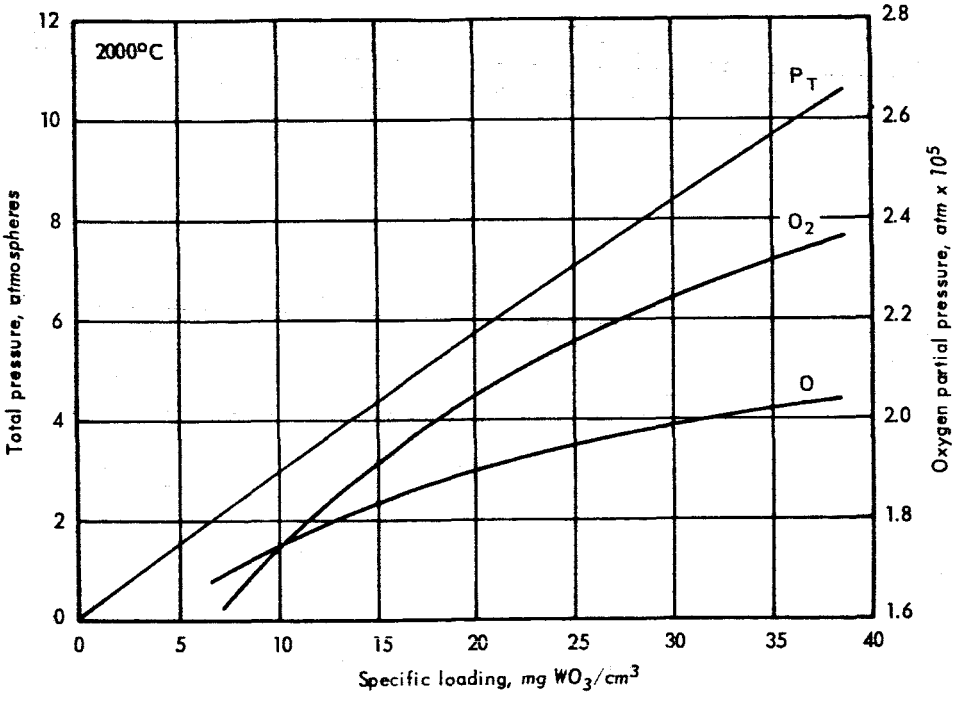

Fig. B1 – Oxygen partial pressure and total pressure ($P_{W_xO_y} + P_O + P_{O_2}$) at 2000°C as a function of capsule loading

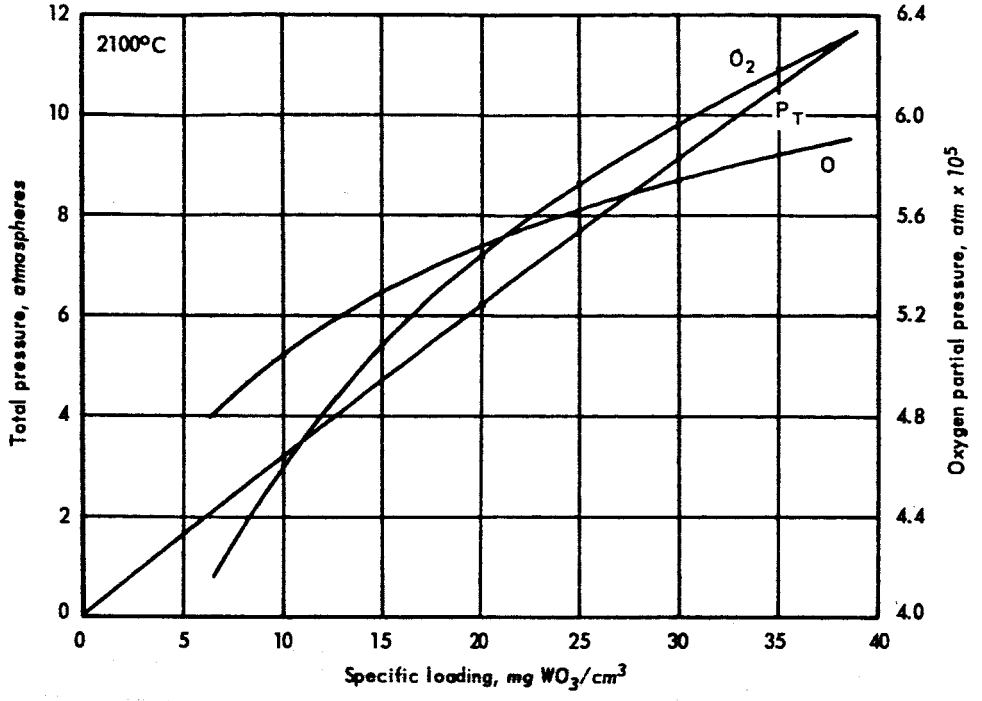

Fig. B2 – Oxygen partial pressure and total pressure ($P_{W_xO_y} + P_O + P_{O_2}$) at 2100°C as a function of capsule loading

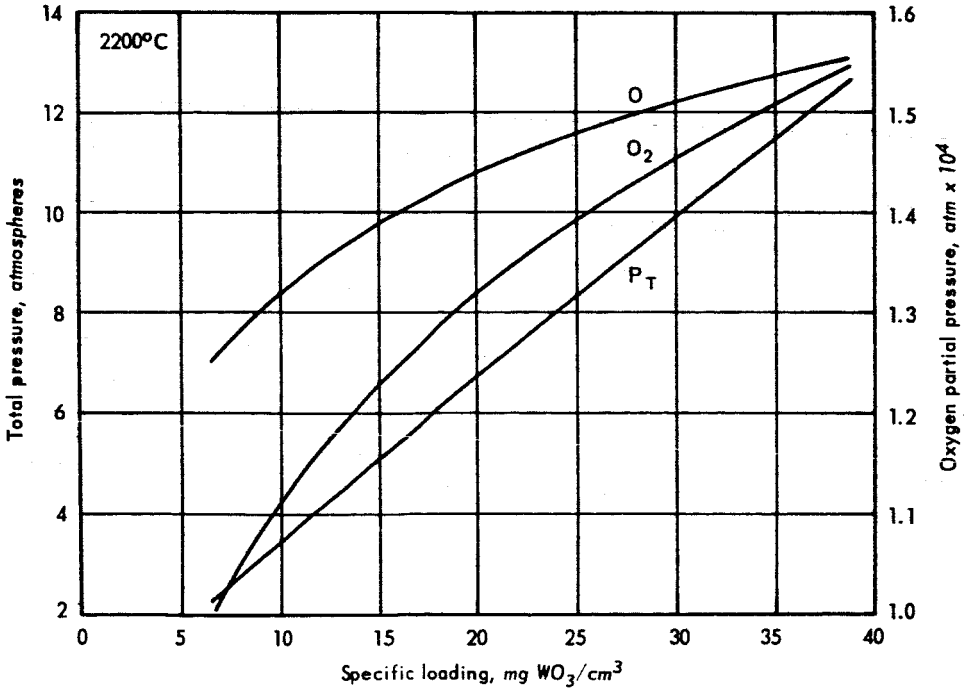

Fig. B3 – Oxygen partial pressure and total pressure ($P_{W_xO_y} + P_O + P_{O_2}$) at 2200°C as a function of capsule loading

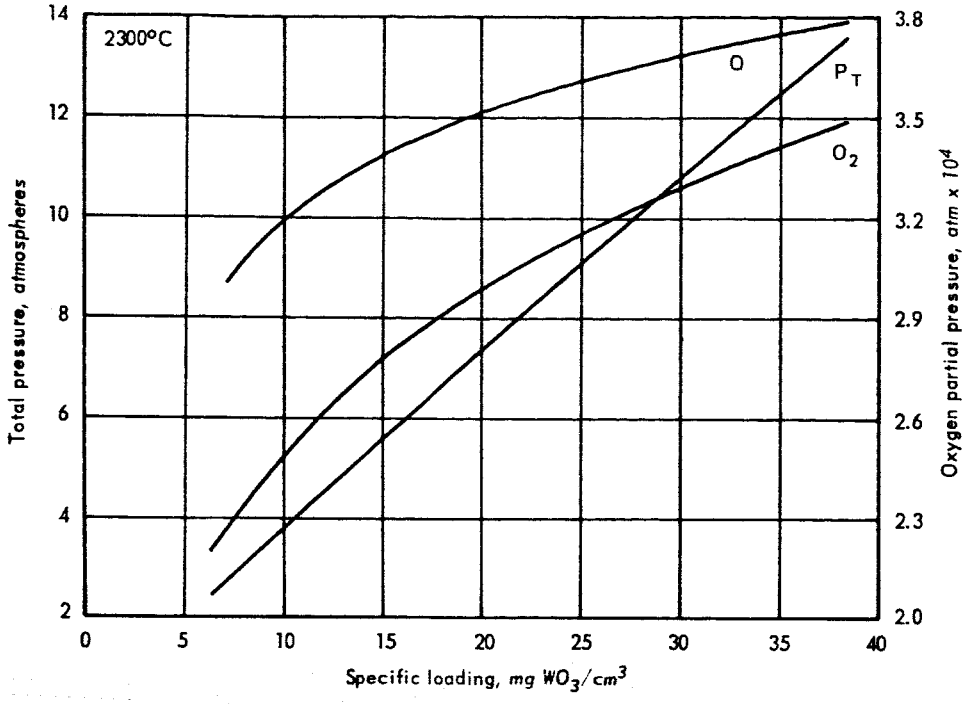

Fig. B4 – Oxygen partial pressure and total pressure ($P_{W_xO_y} + P_O + P_{O_2}$) at 2300°C as a function of capsule loading

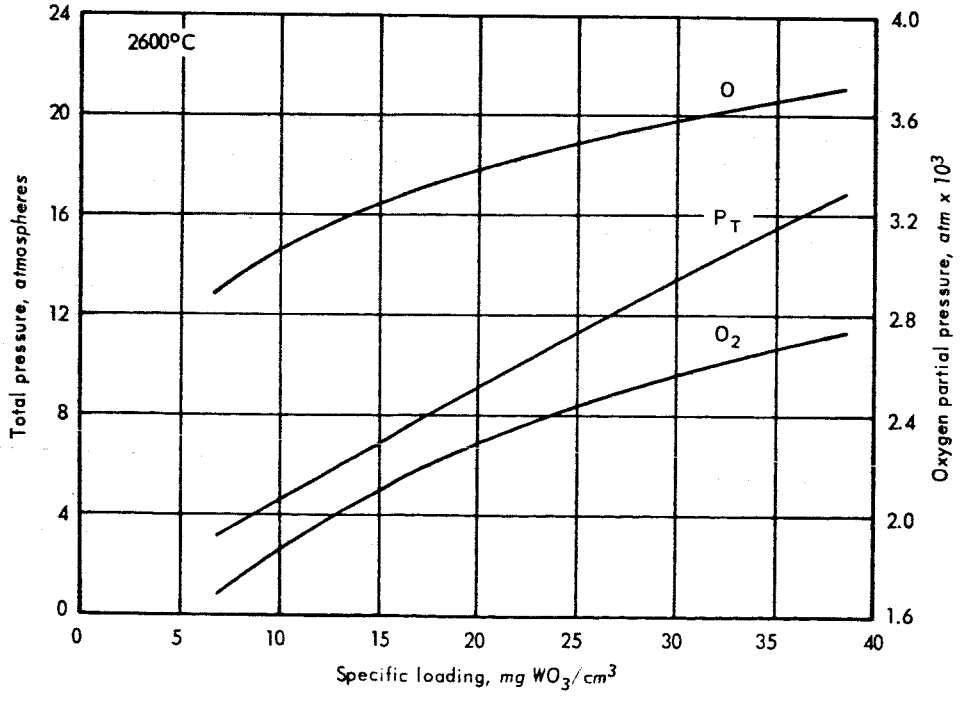

Fig. B5 – Oxygen partial pressure and total pressure ($P_{W_xO_y} + P_O + P_{O_2}$) at 2600°C as a function of capsule loading

APPENDIX C

Sample Calculation of Oxygen Permeation Coefficient

The equation for calculating the permeation coefficient is:

$$P = \frac{qd}{A\,t\left(p_1^{1/2} - p_2^{1/2}\right)}$$

where:

P = temperature dependent permeation coefficient
q = quantity of permeated oxygen in cc (STP)
d = membrane thickness in mm
A = membrane area in cm^2
t = permeation time in min.
p_1 = partial pressure of oxygen inside capsule in atmospheres
p_2 = partial pressure of oxygen outside capsule in atmospheres

Values for q, d, A, t, p_1, and p_2 were obtained as follows.

(Example specimen O-53; see Tables 3 and 4)

$$q = (\text{gms } WO_3)\,(\text{weight fraction oxygen in } WO_3)\,(\text{fraction of oxygen lost})\,\frac{\text{cc } O_2/\text{mole}}{\text{gms } O_2/\text{mole}}$$

$$= 0.1016\left(\frac{48}{232}\right)(0.19)\left(\frac{22,400}{32}\right) = 2.79 \text{ cc (STP)}$$

d = 2.55 mm
A = 15.3 cm^2
t = 180 min

Since the oxygen pressure inside the capsule changed with time during the experiment, the average pressure was used.

$$p_1\,(\text{avg}) = \frac{\text{initial } p_1 + \text{final } p_1}{2}$$

Initial and final oxygen pressures were obtained from Figure B4, knowing initial specific loading of capsule (34.8 mg/cm^3) and final specific loading [(1-fraction lost) (initial loading)] or [(1- 0.19) (34.8)] = 28.2 mg/cm^3.

Therefore, $p_1\,(\text{avg}) = \frac{3.40 \times 10^{-4} + 3.23 \times 10^{-4}}{2} = 3.31 \times 10^{-4}$ atm. Pressure p_2 was assumed to be zero. The oxygen content of the helium was <4 ppm, but past experience has indicated that the refractory metals in intermediate temperature zones of the furnace act as getters to remove most impurities, and probably reduce the oxygen content to lower levels. In addition, permeated oxygen most probably left the capsule surfaces as gaseous

W_xO_y molecules and therefore did not contribute significantly to the oxygen partial pressure of the helium.

On this basis, the permeation coefficient can be expressed as:

$$P = \frac{2.79 \text{ cc (STP)} \times 2.55 \text{ mm}}{15.3 \text{ cm}^2 \times 180 \text{ min} \times (3.31 \times 10^{-4} \text{ atm})^{1/2}} = 0.14 \text{ cc (STP)-mm/cm}^2\text{-min-atm}^{1/2}$$

Using an average oxygen pressure in the capsule is equivalent to connecting two points on the P_{O_2} pressure curve versus specific loading (Figure B4 in the example) with a straight line. While this is not strictly correct, it represents a very small error (1%) in the calculation of the average pressure.

REFERENCES

1. Steigerwald, E. A., "The Permeation of Hydrogen Through Materials for the Sunflower System," TRW, ER-5623, November 15, 1963.
2. Webb, R. W., "Hydrogen Permeation Through Metals," NAA-SR-TDR No. 9844, April 27, 1964.
3. Moore, George E. and Unterwald, F. C., "Thermal Dissociation of Hydrogen," J. Chem. Phys. 40, 2639 (1964).
4. Ryabchikov, L. N., "Mass Spectrometric Investigation of Degasation of Molybdenum, Tungsten, and Niobium on Heating Them in a Vacuum," Ukr. Fiz. Zhur. 9, 293-302 (1964).
5. Jacobs, A. J., "Diffusion of Oxygen in Tungsten and Some Other Transition Metals," Nature, 200, 1310 (1963).
6. Stringer, J. and Rosenfeld, A. R., "Interstitial Solid Solutions in Body-Centred Cube Metals," Nature, 199, 337 (1963).
7. Lee, C. H., "Oxygen Diffusion in Tungsten," Nature, 203, 1163 (1964).
8. Allen, B. C., Maykuth, D. J., and Jaffee, R. I., "The Recrystallization and Ductile-Brittle Transition Behavior of Tungsten," J. Inst. Metals 90, 120 (1961).
9. Atkinson, R. H., Keith, G. H., and Koo, R. C., "Tungsten and Tungsten-Base Alloys" in Refractory Metals and Alloys, Interscience Publishers, New York (1960).
10. Norton, Francis J., "Permeation of Gases Through Solids," J. Appl. Phys. 28, 34 (1957).
11. Stull, D. R. and Sinke, G. C., Thermodynamic Properties of the Elements, Adv. Chem. Series 18, Amer. Chemical Soc., Washington, D. C. (1956).
12. Ang, C. Y., "Activation Energies and Diffusion Coefficients of Oxygen and Nitrogen in Niobium and Tantalum," Acta Met., 1, 123 (1953).
13. Jaffee, R. I., Klopp, W. D., and Sims, C. T., "High-Temperature Oxidation and Contamination of Columbium," Trans. ASM, 51, 282 (1959).
14. Marx, J. W., Baker, G. S., and Siversten, J. M., "The Internal Friction of Tantalum and Columbium Foils at Ultrasonic Frequencies," Acta. Met., 1, 193 (1953).
15. Powers, R. W. and Doyle, M. V., "Diffusion of Interstitial Solutes in the Group V Transition Metals," J. Appl. Phys., 30, 514 (1959).
16. Gulbransen, E. A. and Andrew, K. F., "Kinetics of the Reactions of Columbium and Tantalum with O_2, N_2, and H_2," Trans. AIME, 188, 586 (1950).
17. Gebhardt, E., Seghezzi, H. D., and Stagherr, A., "The Diffusion of Oxygen in Tantalum," Z. Metallk., 48, 624 (1957).
18. Powers, R. W. and Doyle, M. V., "Some Internal Friction Studies in Columbium," Trans. AIME, 209, 1285 (1957).
19. Albrecht, W. M. and Goode, W. D., "Reactions of Nitrogen with Niobium," BMI-1360 (1959).
20. Kreimer, G. S., Efron, L. D., and Voranova, E. A., Zhur, Tekh. Fiz., 22, 858 (1952).
21. Pirani, M. and Sandor, J., "Diffusion of Carbon into Tungsten," J. Inst. Metals, 73, 385 (1947).

22. Wert, C. A., "Measurements on the Diffusion of Interstitial Atoms in B.C.C. Lattices," J. Appl. Phys., 21, 1196 (1950).
23. Kovenski, I. I., "The Investigation of Diffusion of Carbon in Three Refractory Metals Over Wide-Temperature Ranges," paper presented at International Conference on Diffusion in Body-Centered Cubic Metals, held at Gatlinburg, Tennessee, Sept. 16-18, 1964.
24. Albrecht, W. M., Goode, W. D., and Mallett, M. W., "Reactions in the Niobium-Hydrogen System," J. Electrochem. Soc., 106 (11), 981 (1959).
25. Ackermann, R. J. and Rauh, E. G., "A Thermodynamic Study of the Tungsten-Oxygen System at High Temperatures," J. Phys. Chem., 67, 2596, (1963).
26. DeMaria, G., Burns, R. P., Drowart, J., and Inghram, M. G., "Mass Spectrometric Study of Gaseous Molybdenum, Tungsten, and Uranium Oxides," J. Chem. Phys., 32, 1373 (1960).
27. Thorn, R. J. and Ackermann, R. J., "Vaporization of Oxides," Chapter 2 in Progress in Ceramic Science, Vol. 1, Pergamon Press (1961).

DISTRIBUTION

EXTERNAL

NASA Lewis Research Center (6)
21000 Brookpark Road
Cleveland, Ohio 44135
Attention: R. E. Gluyas (105-1)

NASA Lewis Research Center (1)
21000 Brookpark Road
Cleveland, Ohio 44135
Attention: Technical Utilization
Office, M. S. 3-16

NASA Lewis Research Center (2)
21000 Brookpark Road
Cleveland, Ohio 44135
Attention: Library M. S. 60-3

U. S. Atomic Energy Commission (3)
Technical Reports Library
Washington, D. C.

A. E. C. Headquarters (1)
Division of Reactor Development
Washington, D. C.
Attention: J. Simmons

NASA Program Manager (2)
Space Nuclear Propulsion Office
U. S. Atomic Energy Commission
Washington, D. C. 20545
Attention: F. C. Schwenk

NASA Lewis Research Center (1)
21000 Brookpark Road
Cleveland, Ohio 44135
Attention: Office of Reliability
and Quality Assurance

NASA Ames Research Center (1)
Moffett Field, California 94035
Attention: Library

NASA Goddard Space Flight Center (1)
Greenbelt, Maryland 20771
Attention: Library

NASA Lewis Research Center
21000 Brookpark Road
Cleveland, Ohio 44135
Attention: (1 copy to each)
Nuclear Rocket Technology Office, M. S. 501-2
Neal Saunders, M. S. 105-1
S. Kaufman, M. S. 49-2
T. Moss, M. S. 500-309
J. Creagh, M. S. 500-309
H. Smreker, M. S. 501-2
W. Klopp, M. S. 105-1
R. Hall, M. S. 105-1
M. Dustin, M. S. 54-1

NASA Flight Research Center (1)
Post Office Box 273
Edwards, California 93523
Attention: Library

Air Force Materials Lab'y (2)
Wright-Patterson A. F. B.
Dayton, Ohio
Attention: R. L. Prickett (MAMS)

Jet Propulsion Laboratory (1)
4800 Oak Grove Drive
Pasadena, California 9110
Attention: Library

NASA Langley Research Center (1)
Langley Station
Hampton, Virginia 23365
Attention: Library

NASA Marshall Space Flight Center (1)
Huntsville, Alabama 35812
Attention: Library

Argonne National Laboratory (2)
9700 South Cass Avenue
Argonne, Illinois
Attention: J. Schumar
R. Noland

EXTERNAL (Cont.)

NASA Lewis Research Center (1)
21000 Brookpark Road
Cleveland, Ohio 44135
Attention: T. J. Flanagan
Contracting Officer
M. S. 500-210

NASA Lewis Research Center (1)
21000 Brookpark Road
Cleveland, Ohio 44135
Attention: Reports Control
Office (5-5)

NASA Scientific and Technical
Information Facility (6 and
reproducible)
Box 5700
Bethesda, Maryland
Attention: NASA Representative

U. S. Atomic Energy Commission (3)
Technical Information Service Extension
Post Office Box 62
Oak Ridge, Tennessee

National Aeronautics and Space
Administration (1)
Washington, D. C. 20546
Attention: G. C. Deutsch (RRM)

General Electric Company (2)
Vallecitos Atomic Laboratory
Post Office Box 846
Pleasanton, California
Attention: Dr. A. Kaznoff
Dr. E. A. Aitken

NASA Manned Spacecraft Center (1)
Houston, Texas 77001
Attention: Library

NASA Western Operations (1)
150 Pico Boulevard
Santa Monica, California 90406
Attention: Library

Battelle Northwest Labs (2)
Richland, Washington
Attention: F. Albaugh
R. Baker

Oak Ridge Gaseous Diffusion Plant (1)
Oak Ridge, Tennessee
Attention: P. Huber

Battelle Memorial Institute (1)
505 King Avenue
Columbus, Ohio
Attention: E. Hodge

Sylvania Electric Products, Inc. (1)
Chemical and Metallurgical Division
Towanda, Pennsylvania
Attention: M. B. MacInnis

United Nuclear Corporation (1)
5 New Street
White Plains, New York 10601
Attention: Records Management

General Atomic Division (1)
General Dynamics Corporation
Post Office Box 1111
San Diego, California 92112
Attention: Chief, Technical Information
Services

Atomics International Div. (1)
North American Aviation
8900 DeSota Avenue
Canoga Park, California
Attention: S. Carneglia

Nuclear Materials and Equipment
Corporation (1)
Apollo, Pennsylvania
Attention: B. Vondra

Westinghouse Electric Corp. (1)
Astronuclear Laboratory
Box 10864
Pittsburgh, Pennsylvania 15236
Attention: D. Thomas

Union Carbide Corporation (1)
Nuclear Products Department
Lawrenceburg, Tennessee
Attention: W. Eatherly

Martin-Marietta Corporation (1)
Nuclear Division
Baltimore, Maryland 21203
Attention: J. Monroe

INTERNAL

J. Barnard (NTD)
R. W. Brisken
H. C. Brassfield (2)
V. P. Calkins
J. F. Collins
P. K. Conn (2)
J. B. Conway
D. H. Culver
E. C. Duderstadt (2)
R. E. Fryxell (2)
A. B. Greninger (NTD)
G. F. Hamby (5)
L. D. Jordan
G. Korton
J. A. McGurty
J. Moteff
G. T. Muehlenkamp
W. E. Niemuth
G. Pomeroy
F. C. Robertshaw
R. E. Tallman
G. R. VanHouten
O. G. Woike
C. S. Wukusick (MDLO)
Library (6)